FFI RAPPORT

PREDICTION OF CONCRETE PENETRATION USING FORRESTAL'S FORMULA

SJØL Henrik, TELAND Jan Arild

FFI/RAPPORT-99/04415

FFIBM/766/130

Approved
Kjeller 29 June 2000

Bjarne Haugstad
Director of Research

PREDICTION OF CONCRETE PENETRATION USING FORRESTAL'S FORMULA

SJØL Henrik, TELAND Jan Arild

FFI/RAPPORT-99/04415

FORSVARETS FORSKNINGSINSTITUTT
Norwegian Defence Research Establishment
P O Box 25, NO-2027 Kjeller, Norway

FORSVARETS FORSKNINGSINSTITUTT (FFI)
Norwegian Defence Research Establishment

P O BOX 25
N0-2027 KJELLER, NORWAY

UNCLASSIFIED

SECURITY CLASSIFICATION OF THIS PAGE
(when data entered)

REPORT DOCUMENTATION PAGE

1) PUBL/REPORT NUMBER	2) SECURITY CLASSIFICATION	3) NUMBER OF PAGES
FFI/RAPPORT-99/04415	UNCLASSIFIED	48
1a) PROJECT REFERENCE	**2a) DECLASSIFICATION/DOWNGRADING SCHEDULE**	
FFIBM/766/130	-	

4) TITLE

PREDICTION OF CONCRETE PENETRATION USING FORRESTAL'S FORMULA

5) NAMES OF AUTHOR(S) IN FULL (surname first)

SJØL Henrik, TELAND Jan Arild

6) DISTRIBUTION STATEMENT

Approved for public release. Distribution unlimited. (Offentlig tilgjengelig)

7) INDEXING TERMS

IN ENGLISH:	IN NORWEGIAN:
a) Penetration	a) Penetrasjon
b) Empirical formulas	b) Empiriske formler
c) Concrete	c) Betong
d)	d)
e)	e)

THESAURUS REFERENCE:

8) ABSTRACT

The various existing empirical formulas for predicting penetration into concrete targets are seen to give different results. Explaining the difference is difficult since most of the original empirical data behind the various formulas are not available. The range of the parameters used in the experiments is known, though. The theoretical formula developed by Forrestal, based on the cavity expansion theory, seems to be in good agreement with experiments for various projectiles and various quality of the concrete target. Forrestal's formula is analysed using non-dimensional quantities, and this formula is used to analyse the other existing empirical formulas for predicting penetration into concrete. Assuming that Forrestal's formula predicts the penetration depth correctly, least square approximations, and possible "empirical equations" for constant non-dimensional mass are calculated. These "empirical equations" turn out to be very sensitive to the range of the impact velocity used in the experiments. Many existing empirical formulas are based on experiments with different values of length to diameter ratio in their data sets. The resulting empirical formula from such data sets may become "arbitrary". This means that even though the range of the non-dimensional parameters are identical, the resulting empirical formulas turn out to be quite different. From these observations, an explanation of the difference between the empirical formulas is suggested. Finally, Forrestal's formula is applied to different kinds of modern penetrating weapons.

9) DATE	AUTHORIZED BY This page only	POSITION
29 June 2000	Bjarne Haugstad	Director of Research

ISBN-82-464-0436-9

UNCLASSIFIED

SECURITY CLASSIFICATION OF THIS PAGE
(when data entered)

CONTENTS

PREDICTION OF CONCRETE PENETRATION USING FORRESTAL'S FORMULA

1 INTRODUCTION

Many empirical equations exist for predicting the penetration depth in concrete targets. As shown in Teland (21), these formulas give different results, and have a limited range of validity. Explaining the difference is difficult since most of the original empirical data behind the various formulas are not available. The range of the parameters used in the experiments is known, though.

In this report, an explanation will be attempted by comparing the empirical formulas to Forrestal's approach, which has the nice feature of giving good results while being based on physical principles. Some special assumptions will make it possible to suggest explanations for the discrepancy between the formulas.

After some introductory remarks on dimensional analysis and various existing empirical formulas in chapter 2 and 3, Forrestal's formula is examined in Chapter 4. In Chapter 5, it is compared to existing empirical data. In Chapter 6, the most important empirical formulas are compared to Forrestal's formula within their experimental range of parameters. In Chapter 7, Forrestal's formula is applied to different modern weapons.

2 DIMENSIONAL ANALYSIS

The majority of the existing formulas are dimensionally wrong, which either means that the formulas are purely empirical or that some important parameters are not included in the formulas. In Table 2.1, the parameters used in Forrestal's formula are listed, and these parameters are also used in the majority of the empirical equations.

Table 2.1: The quantities used in Forrestal's formula.

Quantity	Description	Dimension
x	Penetration depth	L
d	Diameter of the projectile	L
r	Radius of ogivity	L
m	Mass of the projectile	M
v	Striking velocity	MT^{-1}
σ_c	Compressive strength of concrete	$ML^{-1}T^{-2}$
ρ	Density of concrete	ML^{-3}

From dimensional analysis (Buckingham's π-teorem), see Baker et al (2), 4 non-dimensional quantities can be formed from the quantities in Table 2.1, for example:

$$X = \frac{x}{d} \quad V = \sqrt{\frac{m}{d^3 \sigma_c}} v \quad M = \frac{m}{d^3 \rho_t} \quad N = g(r/d) \tag{2.1}$$

where g is an arbitrary function of r/d. It should be noted that the non-dimensional mass M for a cylindrical geometry is proportional to the length to diameter ratio of the projectile, a parameter which is known to be important in penetration problems.

$$M = \frac{\rho_p \pi d^2 l}{4 \rho_t d^3} = \frac{\pi}{4} \frac{\rho_p}{\rho_t} \frac{l}{d} \tag{2.2}$$

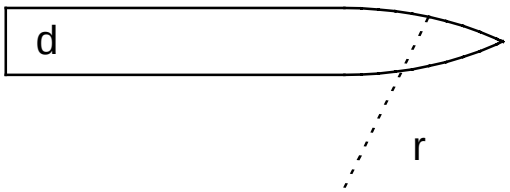

Figure 2.1 Definition of the geometrical parameters for the projectile.

3 EXISTING EMPIRICAL FORMULAS

In Teland (21), the different existing empirical penetration formulas were studied, and the predicted penetration depth was seen to be strongly dependent on the formula used. This is shown in Figure 3.1 for parameters corresponding to penetration of a GBU-28 into normal concrete. The resulting penetration depth when applying different formulas can vary by a factor 2-3, which is a too large uncertainty in the resulting penetration depth.

The empirical equations can be divided into three categories:

- The experimental data are available
- The range of the experimental parameters used is available
- Only the equations are available

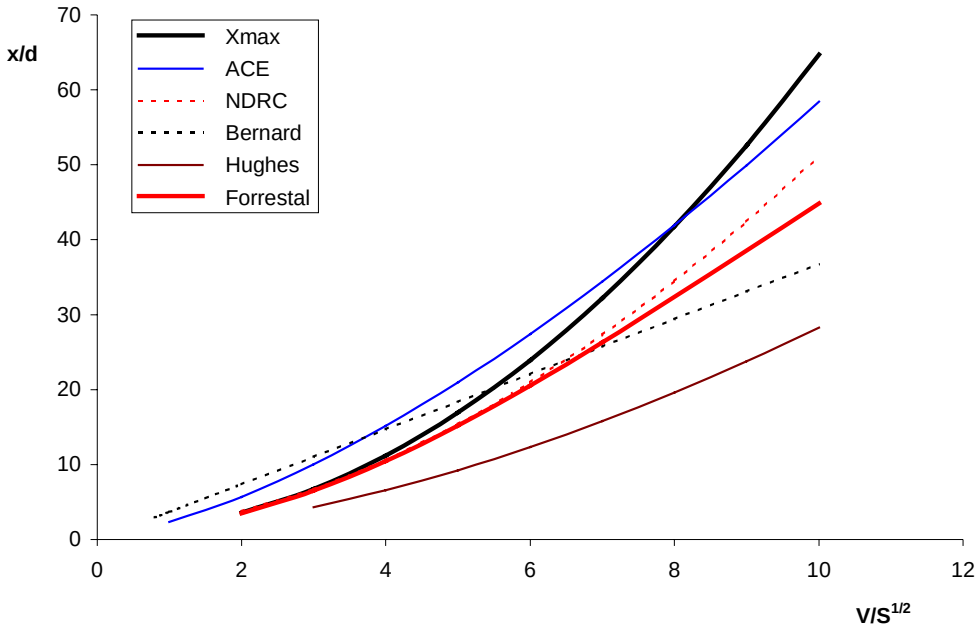

Figure 3.1 Comparison of some different empirical formulas for penetration of GBU-28 into normal concrete.

Most of the formulas shown in Figure 3.1 are used beyond their experimental range. In addition to the formulas shown in Figure 3.1, some other formulas exist. Examples are the Adeli & Amin formula (1) and the Haldar & Miller formula (12), which are only valid for penetration depths less than twice the diameter, and Kar's formula (15), which is a slight correction to the NDRC formula.

4 FORRESTAL'S FORMULA

Forrestal's formula is the only one of the existing empirical formulas that is based upon sound physical principles. The projectile is assumed to be rigid, and the target is semi-infinite. The force acting on the projectile is found from the cavity expansion theory, see Forrestal & Luk (7) and Teland (23). The force decelerating the projectile can be written as

$$f_x = \int_A p_r(u)\cos\theta \, dA\,, \quad u = v\cos\theta \tag{4.1}$$

where v is the projectile velocity, p_r is the radial stress in the target material close to the penetration channel and the integration is performed over the surface area A of the nose. For a simple material model, it is estimated by cavity expansion theory that

$$p_r(v) = A + Bv^2 \tag{4.2}$$

It is then found that A is proportional to the compressive strength of the target material, and B is proportional to the density of the target. The integral in Equation (4.1) gives

$$f_x = \int_A p_r \cos\theta \, dA = \frac{\pi d^2}{4}\left(S\sigma_c + N\rho v^2\right) \qquad x/d > 2 \tag{4.3}$$

The nose factor N is given by

$$N = \begin{cases} \dfrac{8r/d - 1}{24(r/d)^2} & r/d > 1/2 \\ 1 & \text{flat nose} \end{cases} \tag{4.4}$$

and is shown in Figure 4.1.

The penetration depth is then found from Newton's 2nd law:

$$\frac{x}{d} = \frac{2}{\pi}\frac{M}{N}\ln\left[\frac{M/N + \hat{V}^2}{(\pi/2 + M/N)}\right] + 2 \qquad \hat{V} > \sqrt{\frac{\pi}{2}} \tag{4.5}$$

where $\hat{V}^2 = V^2/S$. The derivation of Forrestal's Equation (4.2) is performed in Appendix A.

It is seen that the penetration depth in Forrestal's formula only depends on two non-dimensional parameters; *M/N* and $V/S^{1/2}$. In Section 4.5, it will be shown that the penetration depth is very sensitive to the value of *M/N*.

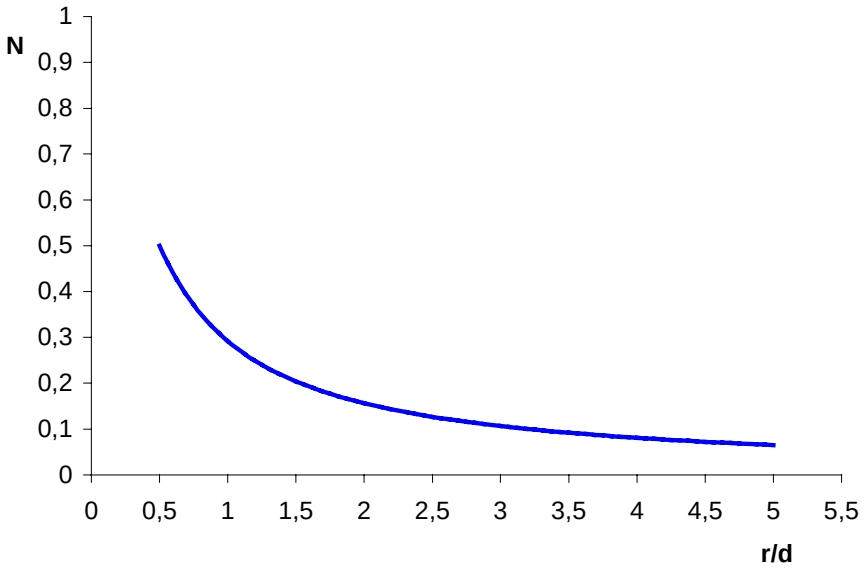

Figure 4.1 The nose factor N as a function of r/d.

4.1 The "S-factor"

From Equation (4.5), the S-factor can be explicitly calculated:

$$S = \frac{N/M\, V^2}{(\pi/2\, N/M + 1)\exp(\pi/2\, N/M\,(X - 2)) - 1} \tag{4.6}$$

From Forrestal's experiments (7), (8), (9), the S-factor is experimentally determined as a function of the compressive strength

$$S = 82.6\left(\frac{\sigma_c}{10^6}\right)^{-0.544} \tag{4.7}$$

where σ_c is measured in SI-units (Pa). The constant S is, by definition, non-dimensional, but the right-hand side of Equation (4.5) does not satisfy this requirement. In principle, S should be on the form

$$S = f\left(\frac{\sigma_c}{p}\right) \tag{4.8}$$

where p has dimension stress. As shown in Section 5.6, when discussing the data behind Bernard's formula, the S-factor calculated for concrete in Equation (4.9), gives inaccurate results when applied to rock targets. This further indicates that the S-factor should depend on other material parameters than the compressive strength as well.

The S-factor as defined by Forrestal in Equation (4.5) is only valid for compressive strengths below 100 MPa. By including some experiments with compressive strengths up to 200 MPa, as well as some other available experiments, a corrected expression for the S-factor was found to be

$$S = 49.5\left(\frac{\sigma_c}{10^6}\right)^{-0.43} \tag{4.9}$$

The new and old S-factors are compared in Figure 4.2 together with the experiments used to determine the corrected S-factor. Figure 4.2 shows that there is larger difference in the experimental determined S-factor for concrete with low compressive strength compared to concrete with large values of σ_c. Forrestal's S-factor and the corrected S-factor for high performance concrete gives approximately the same value.

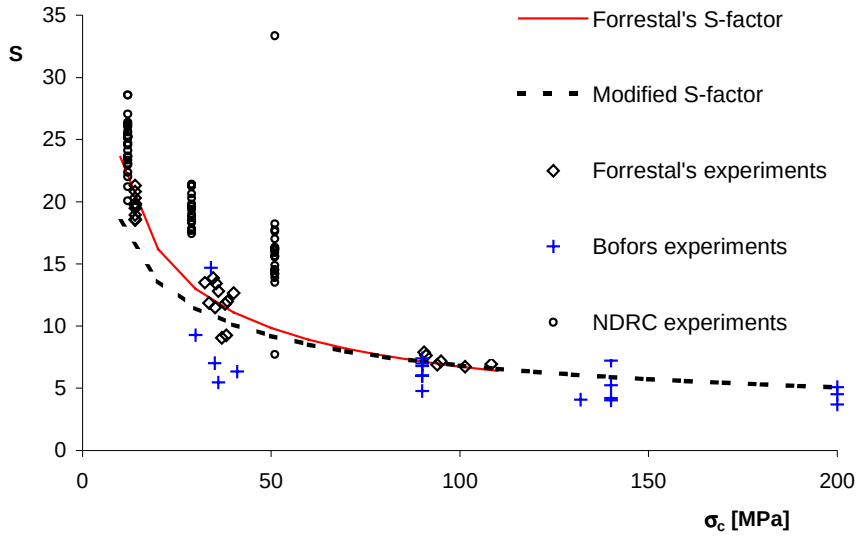

Figure 4.2 Comparison of Forrestal's S-factor to the modified S-factor, and the experimental data behind the modified S-factor.

4.2 Maximum penetration depth

For very long projectiles, the penetration depth as a function of the non-dimensional impact velocity is determined by

$$X_{max} = \lim_{\substack{M/N \to \infty \\ \hat{V}=const}} X = \frac{2}{\pi}\hat{V}^2 + 1 \qquad \hat{V} > \sqrt{\frac{\pi}{2}} \tag{4.10}$$

It should be noted that this is a theoretical limit only, as extremely slender penetrators may break up during the penetration process. (Erosion phenomena are not relevant within this rigid-body approach.)

4.3 Inflection point

Forrestal's formula, as given in Equation (4.5), shows a logaritmic behaviour. For low values of the impact velocity, the penetration depth goes like v^2, which means that there must exist an inflection point, i.e.

$$\frac{\partial^2 X_{max}}{\partial \hat{V}^2} = 0 \tag{4.11}$$

Derivation of Equation (4.5) twice gives

$$\frac{\partial^2 X_{max}}{\partial \hat{V}^2} = \frac{4}{\pi}\frac{M}{N}\frac{M/N - \hat{V}^2}{\left(\hat{V}^2 + M/N\right)^2} \tag{4.12}$$

By solving Equations (4.11) and (4.12), it is found that the inflection point velocity is given by

$$\hat{V}_i = \sqrt{\frac{M}{N}} \tag{4.13}$$

This is schematically shown in Figure 4.3.

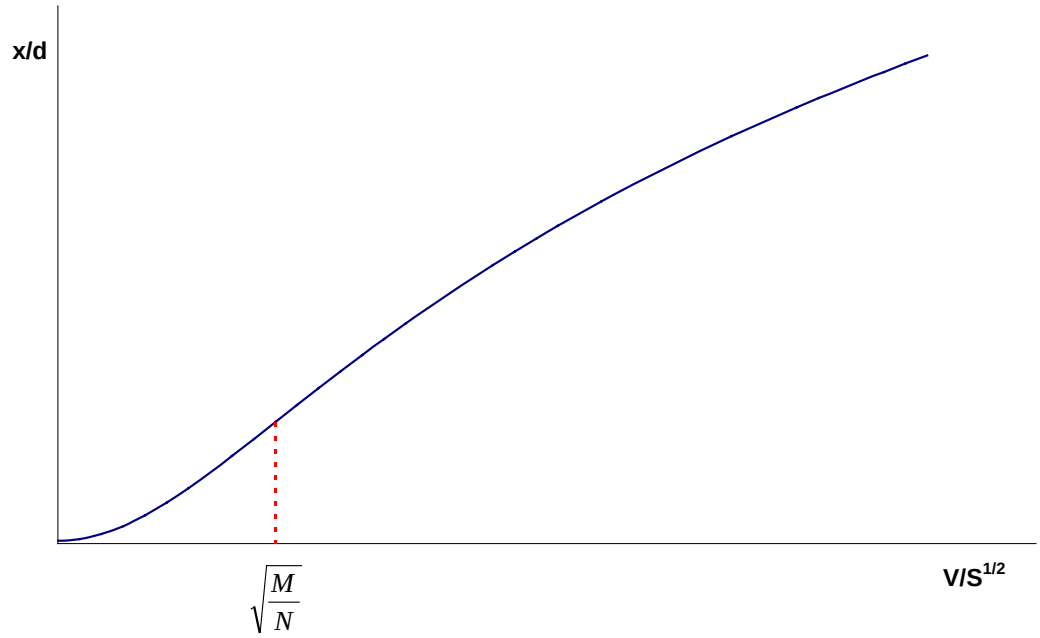

Figure 4.3 The inflection point in Forrestal's formula.

4.4 Flat nosed projectiles

One of the assumptions behind Forrestal's formula is that the force acting on the projectile is given by cavity expansion theory only for penetration depths larger than two calibers. In the first phase of the penetration process, the force is assumed to be proportional to the penetration depth, i.e. the force is increasing linearly from zero to maximum force given by cavity expansion theory. For flat nosed projectiles, the actual force will act almost instantanously on the projectile, without the first phase that exist for ogive nosed projectiles. This assumption will give a modified version of Forrestal's formula

$$\left(\frac{x}{d}\right)_{\text{mod}} = \frac{2}{\pi}\frac{M}{N}\ln\left[1+\frac{N}{M}\frac{V^2}{S}\right] \tag{4.14}$$

The derivation of this formula can be found in Appendix A.

4.5 Variation of M/N

From Equation (4.5), the parameter *M/N* is seen to be important when determining the penetration depth. In Figure 4.4, the non-dimensional penetration depth as a function of non-dimensional impact velocity is shown for different values of *M/N*.

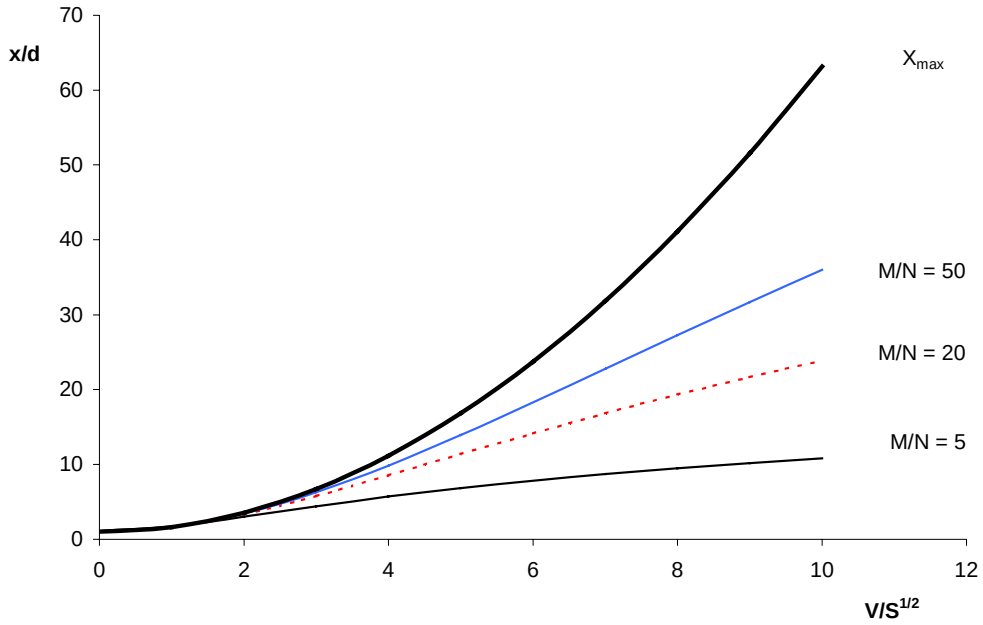

Figure 4.4 Forrestal's formula for different values of M/N.

Figure 4.4 shows a similar difference in penetration depth as the empirical formulas shown in Figure 3.1. This indicates that the different sets of empirical data might have been based upon experiments with different values of M/N. This is further discussed in Chapters 5 and 6.

4.6 General cavity expansion theory

The material model, and hence the expression for the stress in the target material, is simplified in order to calculate the penetration equation analytically. In general, the radial stress p_r is at least dependent on the elastic parameters K and G (bulk and shear modulus, respectively), the porous equation of state $p(\rho)$, and the yield surface $\sigma_y(p)$. This gives a more general expression for the force, as shown in Equation (4.15):

$$f_x = \int_A p_r(K, G, p(\rho), \sigma_Y(p), \ldots) dA \qquad (4.15)$$

The penetration depth based on this general expression of the force will not be studied in this report. Some numerical analysis of the cavity expansion theory using different material models for concrete is discussed in Berthelsen (5).

5 COMPARISON WITH EMPIRICAL DATA

The empirical data behind some of the equations are available, and are in this chapter analysed and compared to Forrestal's formula. In addition some other empirical data are compared to the theoretical model. The experiments are performed with a large range of *M/N* (from 5.6 to 210) and against concrete targets with compressive strengths between 12 and 200 MPa.

5.1 Forrestal's data

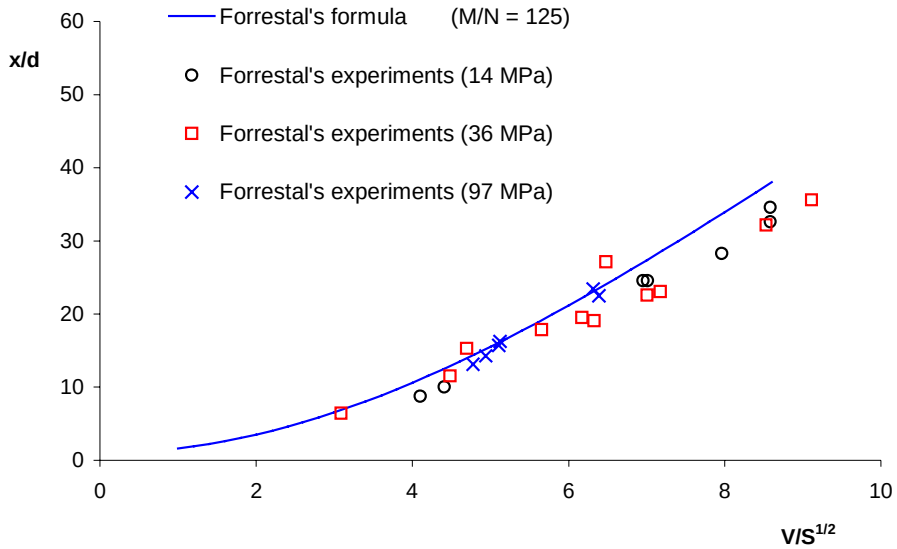

Figure 5.1: Forrestal's formula compared to Forrestal's data.

The experimental data, which Forrestal calculated the S-factor from, is taken from the references (7) – (9). The experiments were performed against concrete targets with compressive strength varying between 14 and 108 MPa. The data are listed in Table 5.1, and are compared to Forrestal's formula in Figure 5.1.

Table 5.1: Empirical data taken from Forrestal's papers (7), (8) and (9).

Comp strength [MPa]	Mass [kg]	Diameter [mm]	Nose factor	M/N	Impact velocity [m/s]	Penetration depth [mm]
14	0.0642	12.7	0.106	151	371	127
14	0.0642	12.7	0.106	151	590	312
14	0.0642	12.7	0.106	151	670	359
14	0.0642	12.7	0.106	151	722	414
14	0.0642	12.7	0.106	151	945	640
14	0.0642	12.7	0.076	210	345	111
14	0.0642	12.7	0.076	210	585	312

14	0.0642	12.7	0.076	210	722	439
14	0.0642	12.7	0.076	210	900	663
35,2	0.906	26.9	0.156	126	277	173
37,8	0.91	26.9	0.156	126	410	310
38,1	0.907	26.9	0.156	126	431	411
33,5	0.912	26.9	0.156	127	499	480
38,4	0.91	26.9	0.156	126	567	525
36,9	0.905	26.9	0.156	126	590	729
40,1	0.901	26.9	0.156	125	591	513
35,4	0.903	26.9	0.156	125	631	607
34,7	0.905	26.9	0.156	126	642	620
36	0.901	26.9	0.156	125	773	866
32,4	0.904	26.9	0.156	126	800	958
90,5	0.907	26.9	0.156	128	561	353
91	0.898	26.9	0.156	126	584	384
95	0.908	26.9	0.156	128	608	422
101,4	0.905	26.9	0.156	127	622	437
94	0.907	26.9	0.156	128	750	630
108,3	0.9	26.9	0.156	127	793	605

5.2 FFI data

In (19), some small scale experiments with flat nosed steel projectiles against concrete targets were reported. Most of these experiments resulted in deformed projectiles, which was due to either high impact velocity or high compressive strength of the concrete targets. Some of the experiments were, however, performed with low impact velocity against standard concrete. The experimental data from these experiments are listed in Table 5.2, and are in Figure 5.2 compared to Forrestal's formula, and the modified formula for flat nosed projectiles (Equation (4.14)). From figure 5.2, it is seen that the modified penetration formula (4.9) gives a better prediction of the penetration depth than the original formula by Forrestal (Equation (4.5)).

Table 5.2: Empirical data taken from the FFI experiments (19) with non-deformed projectiles.

Comp strength [MPa]	Mass [kg]	Diameter [mm]	Nose factor	M/N	Impact velocity [m/s]	Penetration depth [mm]
35	0.0205	12	1	5.6	414	25
35	0.0205	12	1	5.6	445	30

35	0.0205	12	1	5.6	567	37
35	0.0205	12	1	5.6	572	54
35	0.0205	12	1	5.6	749	65
35	0.0205	12	1	5.6	754	53

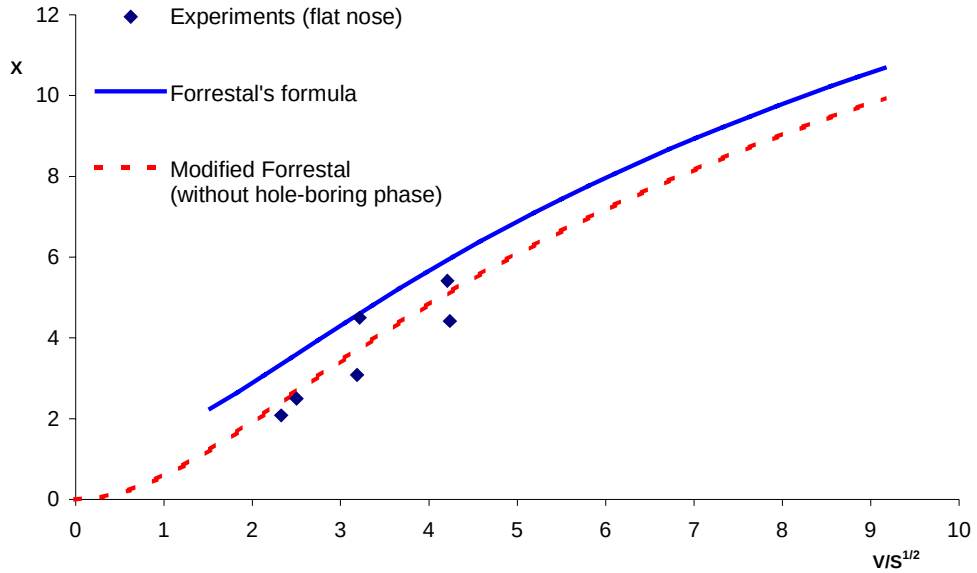

Figure 5.2: Forrestal's formula compared to the FFI data with non-deformed projectiles.

5.3 NDRC data

The NDRC formula is based on 12.7 mm projectiles against various concrete qualities (18). The experimental results are listed in Tables 5.3 – 5.5, and are in Figure 5.3 compared to Forrestal's formula.

Table 5.3: Empirical data taken from experiments behind the NDRC-formula (18) (compressive strength 12 MPa).

Comp strength [MPa]	Mass [kg]	Diameter [mm]	Nose factor	M/N	Impact velocity [m/s]	Penetration depth [mm]
12	0.029	12.7	0.2	32.2	338	76
12	0.029	12.7	0.2	32.2	353	79
12	0.029	12.7	0.2	32.2	368	78
12	0.029	12.7	0.2	32.2	373	95
12	0.029	12.7	0.2	32.2	337	84
12	0.029	12.7	0.2	32.2	338	90
12	0.029	12.7	0.2	32.2	379	95
12	0.029	12.7	0.2	32.2	422	113

12	0.029	12.7	0.2	32.2	437	122
12	0.029	12.7	0.2	32.2	466	144
12	0.029	12.7	0.2	32.2	360	87
12	0.029	12.7	0.2	32.2	513	138
12	0.029	12.7	0.2	32.2	527	167
12	0.029	12.7	0.2	32.2	529	148
12	0.029	12.7	0.2	32.2	544	160
12	0.029	12.7	0.2	32.2	551	162
12	0.029	12.7	0.2	32.2	553	167
12	0.029	12.7	0.2	32.2	351	81
12	0.029	12.7	0.2	32.2	383	90
12	0.029	12.7	0.2	32.2	591	182
12	0.029	12.7	0.2	32.2	632	214
12	0.029	12.7	0.2	32.2	634	207
12	0.029	12.7	0.2	32.2	649	191

Table 5.4: Empirical data taken from experiments behind the NDRC-formula (4) (compressive strength 29 MPa).

Comp strength [MPa]	Mass [kg]	Diameter [mm]	Nose factor	M/N	Impact velocity [m/s]	Penetration depth [mm]
29	0.029	12.7	0.2	32.2	256	35
29	0.029	12.7	0.2	32.2	316	47
29	0.029	12.7	0.2	32.2	323	47
29	0.029	12.7	0.2	32.2	331	50
29	0.029	12.7	0.2	32.2	212	26
29	0.029	12.7	0.2	32.2	233	31
29	0.029	12.7	0.2	32.2	367	53
29	0.029	12.7	0.2	32.2	478	80
29	0.029	12.7	0.2	32.2	491	83
29	0.029	12.7	0.2	32.2	231	28
29	0.029	12.7	0.2	32.2	618	112
29	0.029	12.7	0.2	32.2	671	139
29	0.029	12.7	0.2	32.2	164	21
29	0.029	12.7	0.2	32.2	338	50
29	0.029	12.7	0.2	32.2	368	56

29	0.029	12.7	0.2	32.2	722	143
29	0.029	12.7	0.2	32.2	780	167

Table 5.5: Empirical data taken from experiments behind the NDRC-formula (4) (compressive strength 51 MPa).

Comp strength [MPa]	Mass [kg]	Diameter [mm]	Nose factor	M/N	Impact velocity [m/s]	Penetration depth [mm]
51	0.029	12.7	0.2	32.2	226	23
51	0.029	12.7	0.2	32.2	243	19
51	0.029	12.7	0.2	32.2	337	35
51	0.029	12.7	0.2	32.2	433	58
51	0.029	12.7	0.2	32.2	447	60
51	0.029	12.7	0.2	32.2	210	22
51	0.029	12.7	0.2	32.2	269	30
51	0.029	12.7	0.2	32.2	356	43
51	0.029	12.7	0.2	32.2	496	61
51	0.029	12.7	0.2	32.2	591	83
51	0.029	12.7	0.2	32.2	611	89
51	0.029	12.7	0.2	32.2	369	71
51	0.029	12.7	0.2	32.2	522	71
51	0.029	12.7	0.2	32.2	719	113
51	0.029	12.7	0.2	32.2	734	117
51	0.029	12.7	0.2	32.2	752	120
51	0.029	12.7	0.2	32.2	796	136
51	0.029	12.7	0.2	32.2	346	43
51	0.029	12.7	0.2	32.2	852	157
51	0.029	12.7	0.2	32.2	874	167

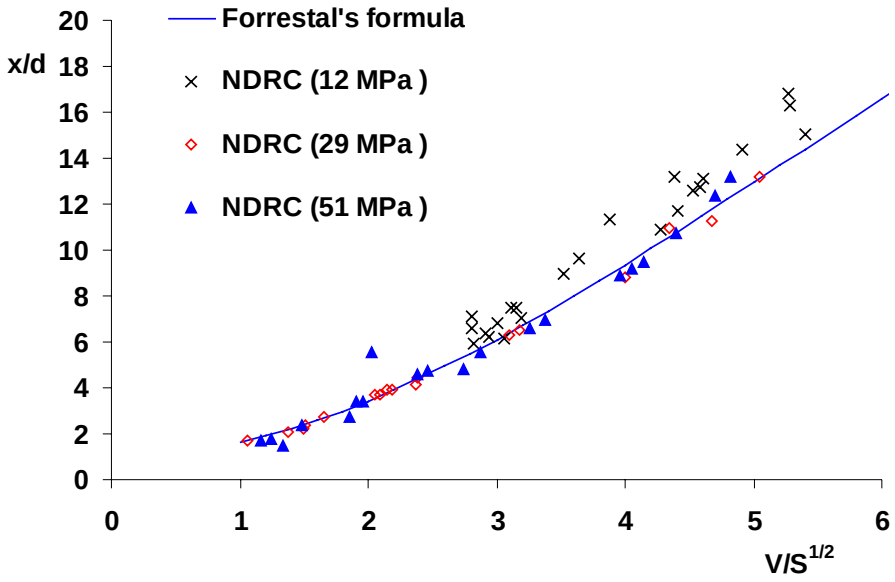

Figure 5.3: Forrestal's formula compared to the NDRC data.

5.4 Bofors data

In the Swedish-Norwegian project on "High Performance Concrete", some penetration experiments against concrete targets with compressive strength varying from 30 to 200 MPa have been performed. The relevant data are listed in Table 5.6 for 152 mm projectiles, and Table 5.7 for 75 mm projectiles.

Table 5.6: Empirical data taken from experiments performed at Bofors with 152 mm projectiles.

Comp strength [MPa]	Mass [kg]	Diameter [mm]	Nose factor	M/N	Impact velocity [m/s]	Penetration depth [mm]
36	44.76	152	0.4	14.5	576	1700
30	44.76	152	0.4	14.5	481	1020
41	44.76	152	0.4	14.5	468	1030
34	44.76	152	0.4	14.5	481	670
90	44.76	152	0.4	14.5	583	980
90	44.76	152	0.4	14.5	479	630
90	44.76	152	0.4	14.5	486	590
90	44.76	152	0.4	14.5	488	560
132	44.76	152	0.4	14.5	581	830
140	44.76	152	0.4	14.5	584	810
140	44.76	152	0.4	14.5	480	595
140	44.76	152	0.4	14.5	480	420

180	44.76	152	0.4	14.5	473	600
200	44.76	152	0.4	14.5	580	530
250	44.76	152	0.4	14.5	481	460
200	44.76	152	0.4	14.5	480	300
203	44.76	152	0.4	14.5	480	450
200	44.76	152	0.4	14.5	480	450
220	44.76	152	0.4	14.5	478	350

Table 5.7: Empirical data taken from experiments performed at Bofors with 75 mm projectiles.

Comp strength [MPa]	Mass [kg]	Diameter [mm]	Nose factor	M/N	Impact velocity [m/s]	Penetration depth [mm]
35	6.28	75	0.2	34	647	990
38	6.28	75	0.2	34	484	680
38	6.28	75	0.2	34	483	655
38	6.28	75	0.2	34	482	660
90	6.28	75	0.2	34	653	560
90	6.28	75	0.2	34	571	410
140	6.28	75	0.2	34	647	440
180	6.28	75	0.2	34	485	250
180	6.28	75	0.2	34	489	235
180	6.28	75	0.2	34	485	240
200	6.28	75	0.2	34	480	200
200	6.28	75	0.2	34	650	440

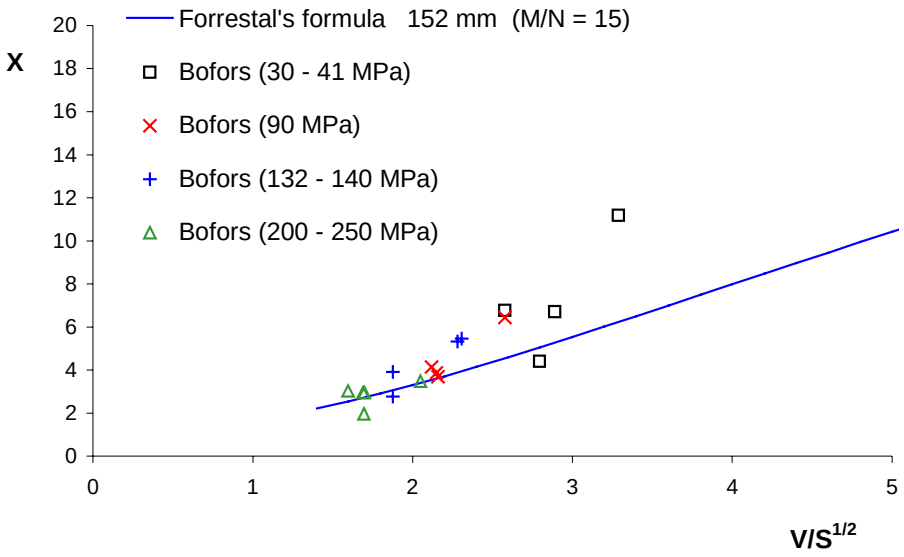

Figure 5.4: Forrestal's formula compared to the Bofors data with 152 mm projectiles.

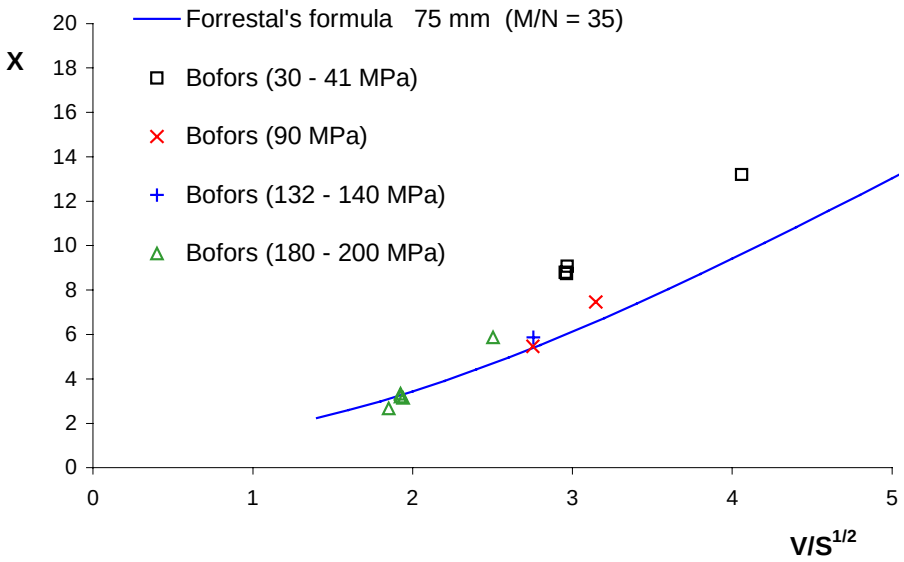

Figure 5.5: Forrestal's formula compared to the Bofors data with 75 mm projectiles.

5.5 Bergman's data

Bergman (3) analysed different experiments to develop his penetration formula. Unfortunately, most of these data can only be found as point in diagrams. This means that there is some uncertainty in the values for impact velocity and penetration depth in Tables 5.8 – 5.14. The value of M/N varies between 25 and 39 in Bergman's experiments, and each test series is compared to Forrestal's formula in Figures 5.6 – 5.12.

Table 5.8: Experiments with 75 mm projectiles (3).

Comp strength [MPa]	Mass [kg]	Diameter [mm]	Nose factor	M/N	Impact velocity [m/s]	Penetration depth [mm]
33.9	5.45	75	0.2	29	160	107
33.9	5.45	75	0.2	29	168	103
33.9	5.45	75	0.2	29	318	222
33.9	5.45	75	0.2	29	329	220
33.9	5.45	75	0.2	29	439	311
33.9	5.45	75	0.2	29	493	332
33.9	5.45	75	0.2	29	493	348
33.9	5.45	75	0.2	29	596	434
33.9	5.45	75	0.2	29	661	506
33.9	5.45	75	0.2	29	685	498
33.9	5.45	75	0.2	29	700	549

Table 5.9: Experiments with 37 mm projectiles (3).

Comp strength [MPa]	Mass [kg]	Diameter [mm]	Nose factor	M/N	Impact velocity [m/s]	Penetration depth [mm]
39.2	0.867	37	0.2	39	233	71
39.2	0.867	37	0.2	39	246	79
39.2	0.867	37	0.2	39	313	114
39.2	0.867	37	0.2	39	317	105
39.2	0.867	37	0.2	39	408	142
39.2	0.867	37	0.2	39	508	188
39.2	0.867	37	0.2	39	517	160
39.2	0.867	37	0.2	39	638	250
39.2	0.867	37	0.2	39	658	265
39.2	0.867	37	0.2	39	700	296
39.2	0.867	37	0.2	39	788	364
39.2	0.867	37	0.2	39	857	463
39.2	0.867	37	0.2	39	857	438
39.2	0.867	37	0.2	39	858	429

Table 5.10: Experiments with 155 mm projectiles (3).

Comp strength [MPa]	Mass [kg]	Diameter [mm]	Nose factor	M/N	Impact velocity [m/s]	Penetration depth [mm]
33	40.2	155	0.2	25	260	330
33	40.2	155	0.2	25	320	400
33	40.2	155	0.2	25	634	980
33	40.2	155	0.2	25	672	1100
33	40.2	155	0.2	25	730	1300

Table 5.11: Experiments with 76 mm projectiles (3).

Comp strength [MPa]	Mass [kg]	Diameter [mm]	Nose factor	M/N	Impact velocity [m/s]	Penetration depth [mm]
35	6.81	76	0.2	35	254	177
35	6.81	76	0.2	35	296	215
35	6.81	76	0.2	35	471	437
35	6.81	76	0.2	35	638	627
35	6.81	76	0.2	35	704	754

Table 5.12: Experiments with 307 mm projectiles (3).

Comp strength [MPa]	Mass [kg]	Diameter [mm]	Nose factor	M/N	Impact velocity [m/s]	Penetration depth [mm]
38.6	454	307	0.2	36	295	1140
38.6	454	307	0.2	36	305	1060
38.6	454	307	0.2	36	305	1150
38.6	454	307	0.2	36	310	1150

Table 5.13: Experiments with 11 mm projectiles (3).

Comp strength [MPa]	Mass [kg]	Diameter [mm]	Nose factor	M/N	Impact velocity [m/s]	Penetration depth [mm]
30.2	0.02	11	0.2	34	280	19
30.2	0.02	11	0.2	34	575	56

30.2	0.02	11	0.2	34	575	64
30.2	0.02	11	0.2	34	595	56
30.2	0.02	11	0.2	34	600	59

Table 5.14: Experiments with 12,7 mm projectiles (3).

Comp strength [MPa]	Mass [kg]	Diameter [mm]	Nose factor	M/N	Impact velocity [m/s]	Penetration depth [mm]
46.3	0.0291	12.7	0.2	32	260	24
46.3	0.0291	12.7	0.2	32	388	36
46.3	0.0291	12.7	0.2	32	446	47
46.3	0.0291	12.7	0.2	32	575	61
46.3	0.0291	12.7	0.2	32	692	85
46.3	0.0291	12.7	0.2	32	788	106
46.3	0.0291	12.7	0.2	32	908	127

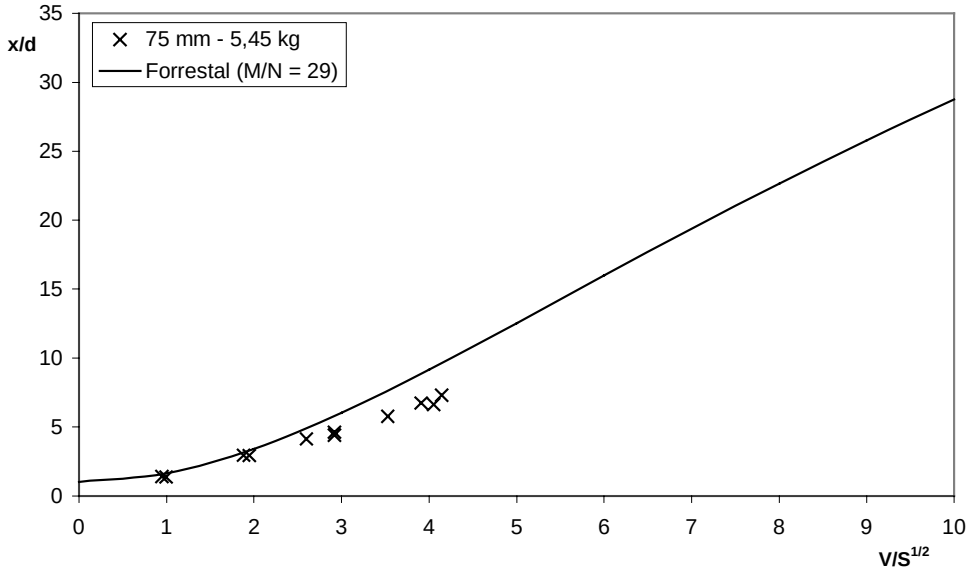

Figure 5.6: Experiments with 75 mm projectiles (3) compared to Forrestal's formula.

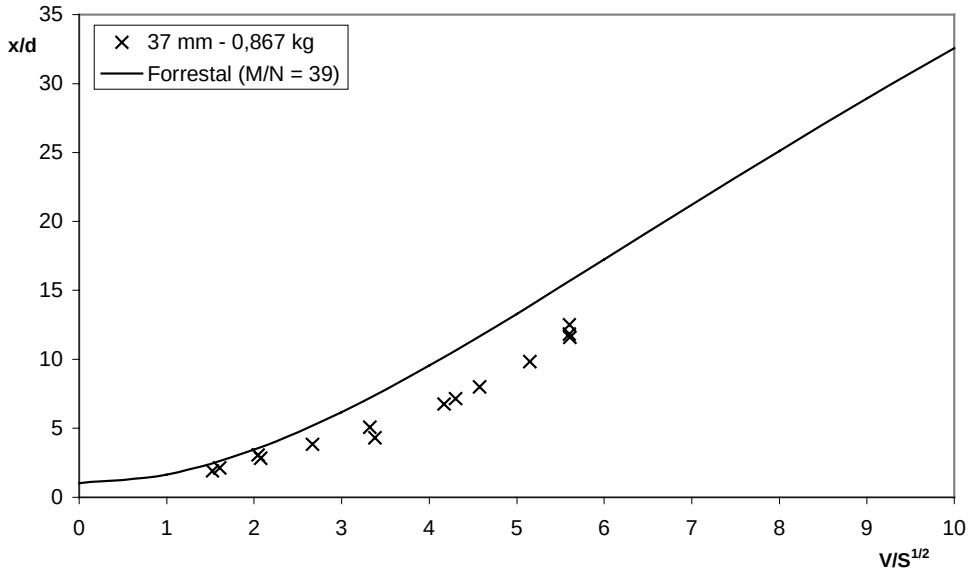

Figure 5.7: Experiments with 37 mm projectiles (3) compared to Forrestal's formula.

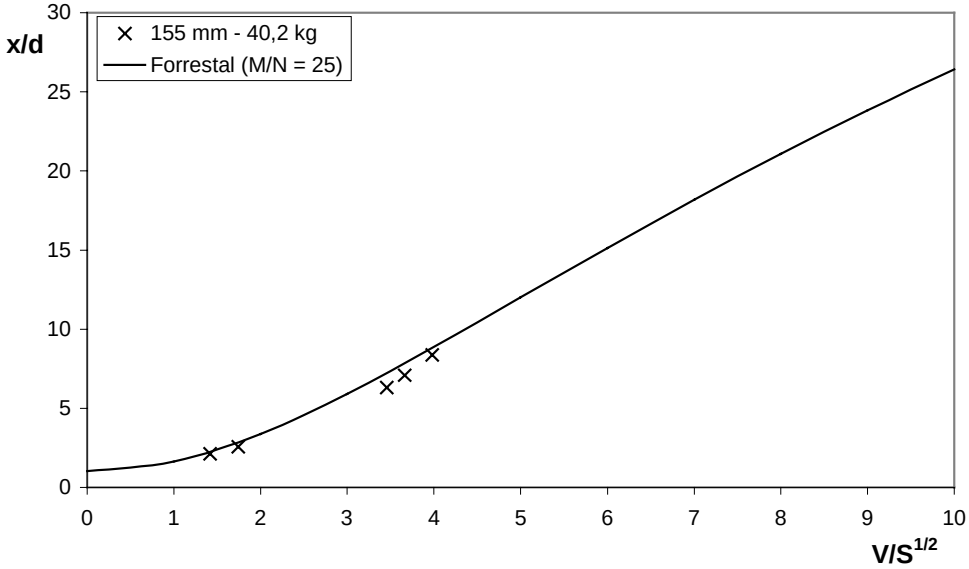

Figur 5.8 Experiments with 155 mm projectiles (3) compared to Forrestal's formula.

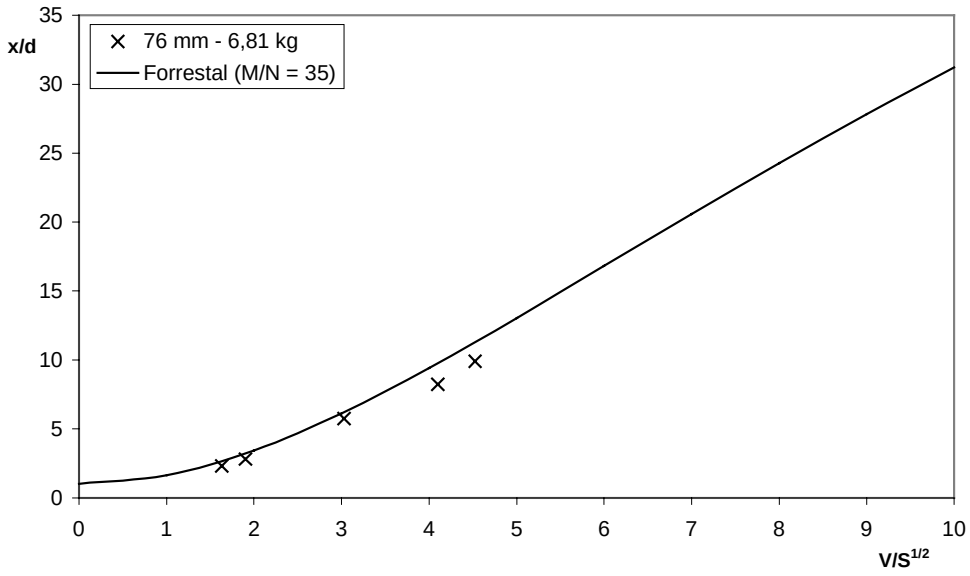

Figure 5.9: Experiments with 76 mm projectiles (3) compared to Forrestal's formula.

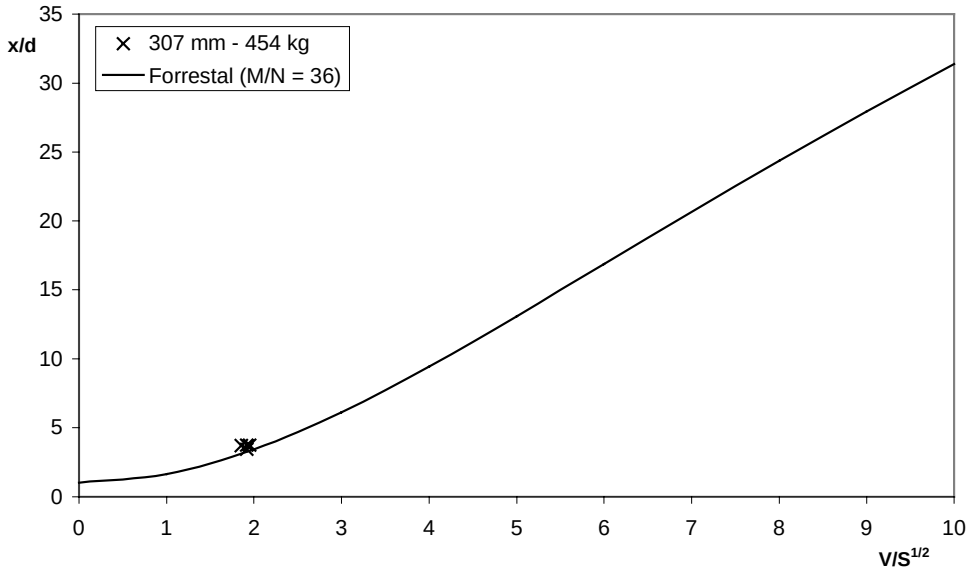

Figure 5.10: Experiments with 307 mm projectiles (3) compared to Forrestal's formula.

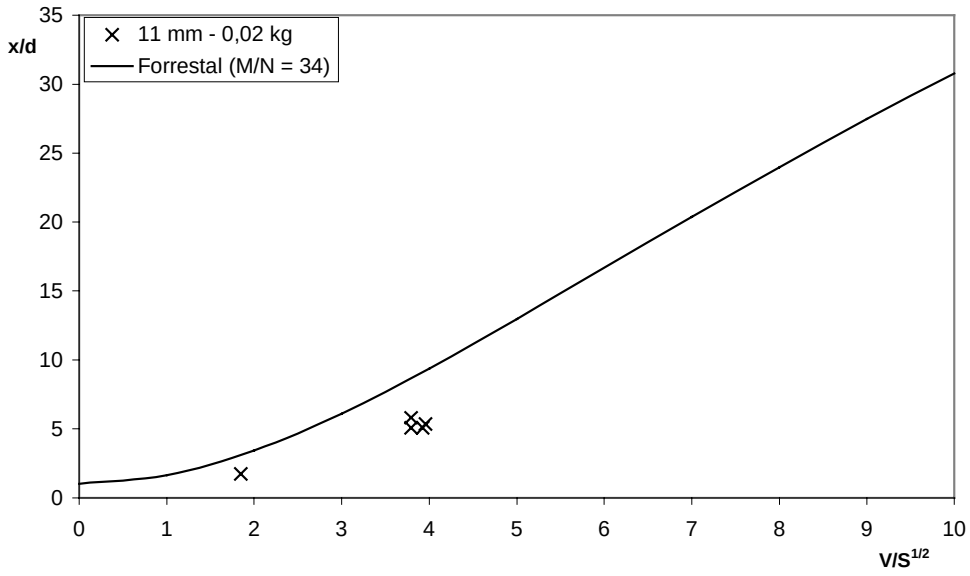

Figure 5.11: Experiments with 11 mm projectiles (3) compared to Forrestal's formula.

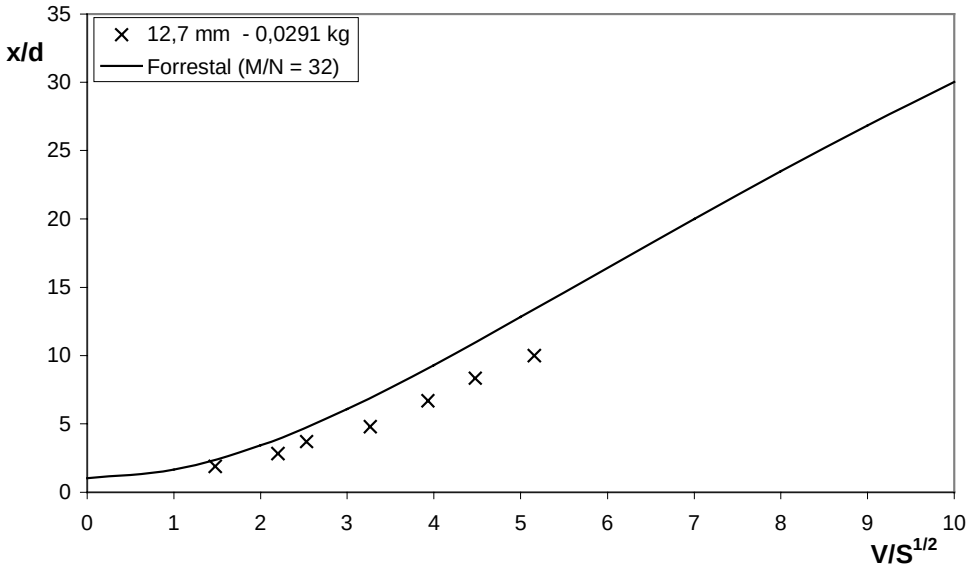

Figure 5.12: Experiments with 12.7 mm projectiles (3) compared to Forrestal's formula.

5.6 Bernard's data

In Bernard (4), some experiments against normal concrete and rock targets were reported. The data from these experiments are listed in Tables 5.14 and 5.15, and are compared to Forrestal's formula in Figure 5.13. All experimental data points in this figure are calculated using the modified S-factor (4.9), which is designed for concrete targets. As seen in Figure 5.13, the experimental data does not fit the Forrestal curve for rock targets. Hence, the S-factor must depend on other material parameters than the compressive strength, as indicated in Equation (4.8).

Table 5.14: Experimental data with 76.2 mm projectiles (4) against normal concrete.

Comp strength [MPa]	Mass [kg]	Diameter [mm]	Nose factor	M/N	Impact velocity [m/s]	Penetration depth [mm]
34.5	5.9	76.2	0.2	28	306	203
34.5	5.9	76.2	0.2	28	312	229
34.5	5.9	76.2	0.2	28	381	254
34.5	5.9	76.2	0.2	28	453	369
34.5	5.9	76.2	0.2	28	541	419
34.5	5.9	76.2	0.2	28	602	597
34.5	5.9	76.2	0.2	28	616	495
34.5	5.9	76.2	0.2	28	709	660
34.5	5.9	76.2	0.2	28	716	610
34.5	5.9	76.2	0.2	28	741	698
34.5	5.9	76.2	0.2	28	773	737
34.5	5.9	76.2	0.2	28	809	749

Table 5.15: Experimental data from Bernard (4) against rock targets.

Compressive strength [MPa]	Mass [kg]	Diameter [mm]	Nose factor	M/N	Impact velocity [m/s]	Penetration depth [mm]
60	208	165.1	0.2	119	372	2220
60	208	165.1	0.2	119	411	2590
60	208	165.1	0.2	119	475	3600
60	208	165.1	0.2	119	501	3350
60	208	165.1	0.2	119	503	3350
23.4	208	165.1	0.2	111	444	3570
23.4	208	165.1	0.2	111	459	3720
27.5	390	228.6	0.2	185	325	3960
48.9	1166	258.8	0.2	156	251	3110
40.8	613	203.2	0.2	171	268	3050
46.2	613	203.2	0.2	139	262	3810

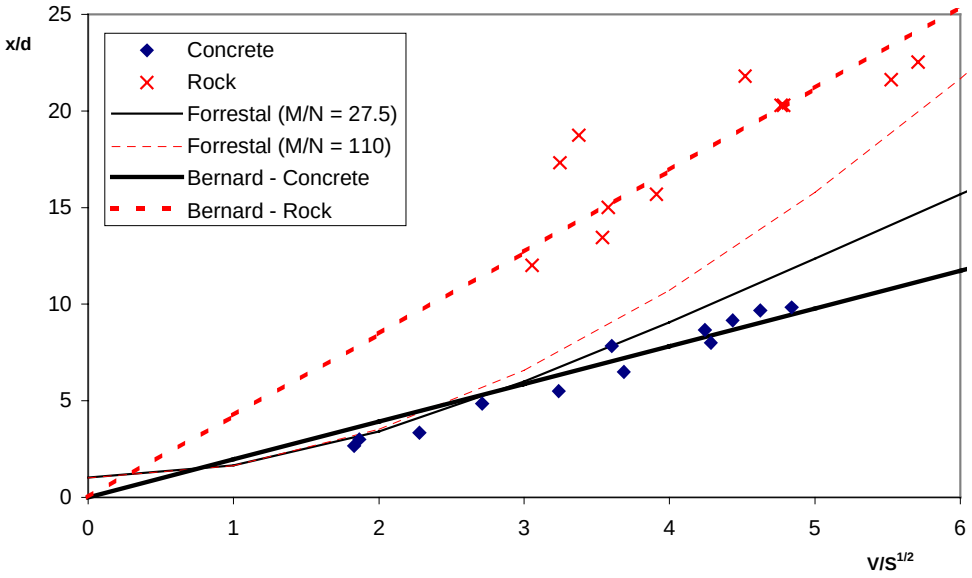

Figure 5.13: Bernard's data compared to Forrestal's and Bernard's formulas.

6 DISCUSSION OF EMPIRICAL FORMULAS

For the majority of the empirical formulas, the original data which the formulas are based on, are not available. However, the range of validity for some of the important parameters is known, and in the present chapter, the value of *M/N* is estimated from the range for the mass and diameter for the projectile. For convenience, the nose-factor, as defined by Forrestal, is set equal to 0.2 when calculating *M/N*.

As shown in Teland and Sjøl (24), most of the existing empirical formulas for predicting penetration into concrete can be written on the form

$$X = a'V^n + b \tag{6.1}$$

where *a'*, *b* and *n* are "constants". The "constants" are not really constants, because the empirical formulas are not dimensionally correct, and when introducing the non-dimensional impact velocity *V*, the "constants *a'*, *b* and *n* may depend on some parameters with dimension. In this document, the non-dimensional impact velocity *V* in Equation (6.1) will be replaced by $\hat{V}$, giving

$$X = g(\hat{V}) = a\hat{V}^n + b \tag{6.2}$$

where *a* is another "constant" which, together with *b* and *n*, is defined in Table 6.1 for the empirical formulas analysed in this report. In Table 6.2, the range of the parameters used in the experiments behind the various empirical formulas ae listed.

Table 6.1: The parameters a, b, and n for different empirical formulas

Formula	**n**	**a**	**b**
ACE [10]	1.5	$0{,}562 N_A \rho^{0{,}25} d^{0{,}165} \sigma_c^{-0{,}073}$	0.5
Bergman [11]	$1.44 + {}^{0.18}\!/_{z} + 0.005z$	$3.68 \cdot 10^{-4} \cdot 137^n \rho^{1-0.5n} d^{0.2} \sigma_c^{0.285n-0.5} N_B M^{1-0.5n}$	0
Bernard [12]	1.0	$34.8\sqrt{M}\sigma_c^{-0.215}$	0
NDRC [13]	1.8	$0.27 N_N d^{0.1} \rho^{0.1} \sigma_c^{0.01} M^{0.1}$	1.0
TBAA [14]	$97.51\sigma_c^{-0.25}$	$2.6104 \cdot 0.257^n ({}^{d}\!/_{c})^{0.1} \sigma_c^{0.285n-0.5} M^{1-0.5n}$	0
Young [15]	1.0	$0.0409 N_Y (11-p) k \rho^{0.2} d^{-0.3} \sigma_c^{-0.015} M^{0.2}$	
		$9.06 \cdot 10^{-3} N_Y (11-p) k \rho^{0.7} d^{-0.3} \sigma_c^{-0.3} M^{0.72}$	

Table 6.2: Range of validity for different empirical formulas.

Formula	**v [m/s]**	**m [kg]**	**d [mm]**	**σ_c [MPa]**
ACE	200 - 1000	0.02 – 454	11 - 155	26.5 - 43.1
Bergman	200 - 1000	0.02 – 454	11 - 305	26.5 - 43.1
Bernard	300 - 800	5.9 - 1066	76.2 - 259	34.5 - 63
Hughes	27 - 1050	0.1 - 343	30 - 305	22.1 - 49.1
TBAA	< 1030	0.14 - 9975	13 - 960	5.5 - 69.1
Young	61 - 1350	3.17 - 2267	25.4 - 762	14 – 63

6.1 Least square approximation

Since the experimental data behind some of the empirical equations are unknown to us, least square approximations to Forrestal's formula will be made instead. As shown in Section 4.5, each value of *M/N* gives different relationships between the penetration depth and the impact velocity. In Section 6.1.1, it is assumed that *M/N* is constant, and we try to calculate the equation on the form (2) that best fits the corresponding "Forrestal curve" for a given impact velocity range.

If an empirical equation is based on experiments with different values of *M/N*, the example in Section 6.1.2 will show that identical range of scaled parameters does not necessarily result in identical empirical equations.

6.1.1 Constant value of M/N

A least square approximation on the form

$$X = g(\hat{V}) = a\hat{V}^n + b \qquad \hat{V} \in [\hat{V}_1, \hat{V}_2] \qquad M/N = \text{constant} \tag{6.3}$$

will be calculated as a best fit to a given ”Forrestal-curve”.

From Table 6.2, it is seen that some of the empirical formulas are based on a large range of the parameters. However, it is reasonable to believe that the small masses and small diameters, and the large masses and large diameters correspond to each other. In addition, the nose factor *N* in Forrestal’s formula is assumed to be *N* = 0.2, which corresponds to a nose with *r/d* = 1.5. With this assumption, the range of the parameter *M/N* and the inflection point velocity can be calculated.

In this analysis, all performed experiments with unavailable data are assumed to agree exactly with Forrestal’s formula. In the actual experiments, there will surely have been some scattering, resulting in some data points lying above or below the assumed value. Neglecting this is not expected to cause significant errors in the analysis.
Assume that the penetration depth as a function of the impact velocity can be written on the form given by Equation (6.3). The least square error between the ”empirical formula” *g* and Forrestal’s formula *f* can be written as

$$E = \int_{\hat{V}_1}^{\hat{V}_2} \left[f(\hat{V}) - g(\hat{V}) \right]^2 d\hat{V} \tag{6.4}$$

where $[\hat{V}_1, \hat{V}_2]$ is the range of impact velocity for the actual formula. By minimizing the error, the constants *a*, *b* and *n* are found to be:

$$a = \frac{F_0 V_n - (\hat{V}_2 - \hat{V}_1) F_n}{V_n^2 - (\hat{V}_2 - \hat{V}_1) V_{2n}} \qquad b = \frac{F_n V_n - F_0 V_{2n}}{V_n^2 - (\hat{V}_2 - \hat{V}_1) V_{2n}} \qquad n = n(\hat{V}_2; \hat{V}_1, M/N) \tag{6.5}$$

where

$$F_n = \int_{\hat{V}_1}^{\hat{V}_2} f(\hat{V}) \hat{V}^n d\hat{V} \quad V_n = \int_{\hat{V}_1}^{\hat{V}_2} \hat{V}^n d\hat{V} \tag{6.6}$$

The velocity exponent *n* which minimizes the least square error must be calculated numerically, and is shown as a function of the range of non-dimensional impact velocity in Figure 6.1. It is seen that the velocity exponent giving the best fit may vary from 0.6 to 3.0 depending on the range of the non-dimensional impact velocity. Especially, if the impact velocity for all experiments are below the inflection point velocity given by Equation (4.13), the velocity exponent is very sensitive to the impact velocity range, and can take almost every value between 1 and 3. If, however, the velocity range includes impact velocities larger than the inflection velocity, the exponent will be between 1.0 and 1.7.

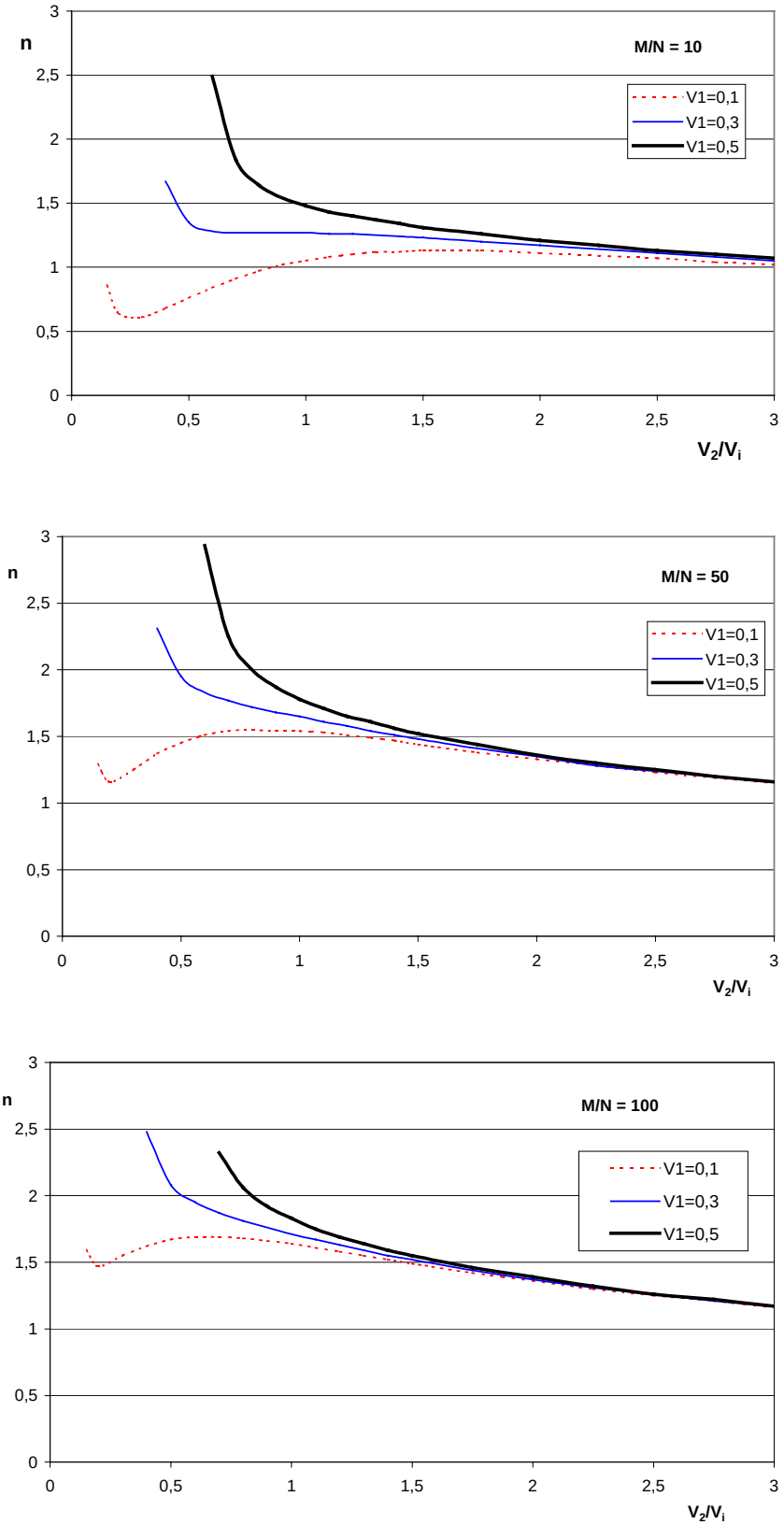

Figure 6.1: The velocity exponent n as a function of the upper range for the impact velocity.

In Figure 6.1 it is seen that for formulas based on a large range of scaled impact velocities, the velocity exponent is close to 1.0, i.e. a linear relationship between the penetration depth and the impact velocity. For experimental data with impact velocities below the inflection

point, the velocity exponent is very sensitive to the range of validity. The non-dimensional impact velocity relative to the inflection point is given by

$$\frac{\hat{V}}{\hat{V}_i} = \sqrt{\frac{N\rho_t}{S\sigma_c}}v \qquad (6.7)$$

This means that the scaled range of validity for the impact velocity does not depend on the projectile size, but only on the compressive strength of the concrete target. Some of the formulas analysed in this report have a large range of validiy for the compressive strength, and we will show below that this can influence the least square approximation.

Table 6.3: Least square approximations.

Formula	$\mathbf{V_{min}/V_i}$	$\mathbf{V_{max}/V_i}$	**n (least square)**	**n (formula)**
ACE	0.2	1.0 – 1.2	1.51 – 1.54	1.5
Bergman	0.2	1.0 – 1.2	1.51 – 1.55	> 1.5
Bernard	0.3	0.7 – 0.9	1.59 – 1.90	1
Hughes	0.03	1.0 – 1.3	1.37	-
NDRC	0.18	0.95	1.51	1.8
TBAA	0	0.9 – 1.9	1.27 – 1.39	1-2
Young	0.1	1.2 – 1.9	1.16 – 1.64	1

6.1.2 Example

To show that different velocity ranges can result in different empirical formulas, different subsets of the NDRC data have been analysed. The NDRC experiments have all been performed with the same projectile with *M/N* = 31.9. In Figure 5, the resulting empirical formulas are shown, and compared to Forrestal's formula for the actual NDRC projectile. The velocity exponent can vary from 1.5 to 1.8, depending on the velocity range.

The prediction of the penetration depth based on these "empirical formulas" is not very different from each other, provided the projectile and target parameters from the NDRC experiments are used. For other values of input parameters, especially with different values of *M/N*, these "empirical" equations may result in wrong predictions of the penetration depth. For a projectile with m = 400 kg, d = 0.155 m and v = 1000 m/s against normal concrete, which is completely different from the NDRC projectile, the penetration depth varies between 12 m and 18 m, depending on which empirical equations from the subsets of the NDRC data is used.

6.1.3 Different values of M/N

Many formulas are based on experiments with different values of *M/N*. As shown in Chapter 4, different values of *M/N* give different formulas for the penetration depth. If empirical formulas are based on such experiments, the resulting empirical formula is very sensitive to the combination of the different parameters. This is illustrated by the following example:

Suppose that experiments are performed with two different values of M/N, say 10 and 100. In Figure 6.2, some fictive data points are shown. The data points "A" result from experiments with *M/N* = 10, the data points "B" from experiments with *M/N* = 100. In addition, the data points "C1" correspond to M/N = 100 and "C2" to *M/N* = 10. If the data points "A", "B" and "C1" are used to construct an empirical formula, a curve close to Forrestal's curve for *M/N* = 100 will arise. If the data points "C1" are substituted by the points "C2", the resulting empirical formula will be equal to Forrestal's formula for M/N = 10. In both cases, the range of the parameters used are idendical, but the resulting empirical formulas give different predictions of the penetration depth.

This analysis indicates that if the span of the parameter *M/N* is large, the resulting formula is determined by the experiments with the highest value of the scaled impact velocity. Since it is not determined by the range of the parameters alone, the formula is therefore in some sense "arbitrary".

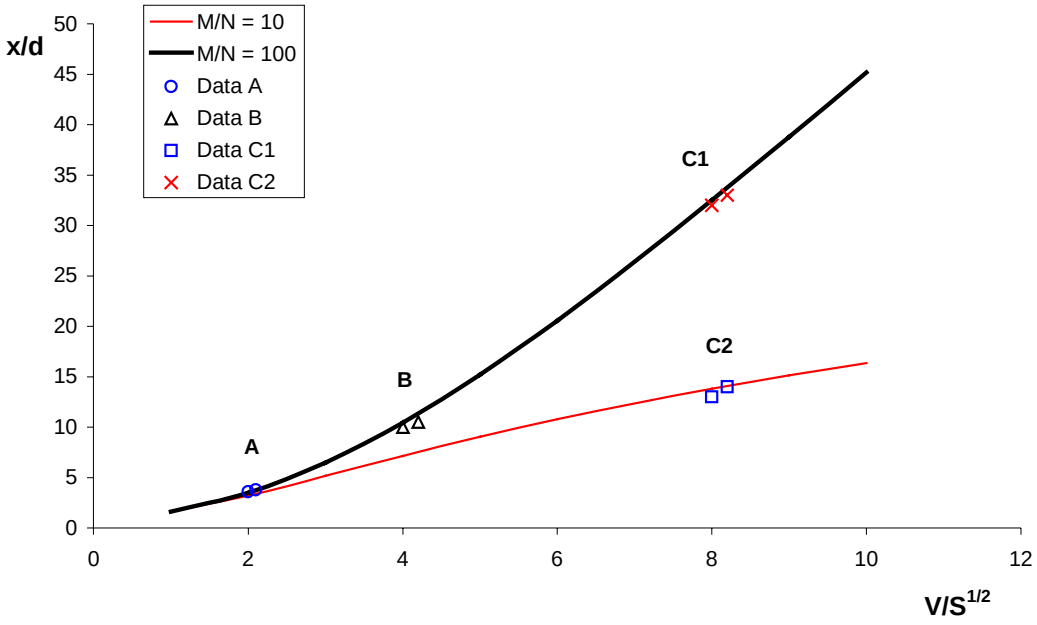

Figure 6.2: Data points from experiments with different values of M/N.

6.2 Comparison between Forrestal's formula and some empirical formulas

We will now look more closely at the individual formulas, and try to explain their difference. Unfortunately, this analysis can not be completed without the data behind all

the empirical formulas. For some of the formulas discussed below, we have the data available, and can therefore compare the present analysis with the actual empirical data. In the Figures 6.3 – 6.8, the solid lines for the relative error are within the range of impact velocity, while the dotted lines indicate the error when the formulas are used outside their range of the impact velocity.

6.2.1 ACE formula

The ACE-formula is not sensitive to the compressive strength, as the penetration depth is proportional to $\sigma_c^{-0.07}$, as shown in Table 1.

The deviation from Forrestal's formula is less than 20 % within the range of the impact velocity for both small and large projectiles. The ACE formula is based on the same experimental data as Bergman's formula, and the value of the parameter *M/N* does not vary much in this data set, see the discussion below for Bergman's formula.

The velocity exponent for the ACE-formula is 1.5, which is also in good agreement with the least square approximation, as shown in Table 6.2.

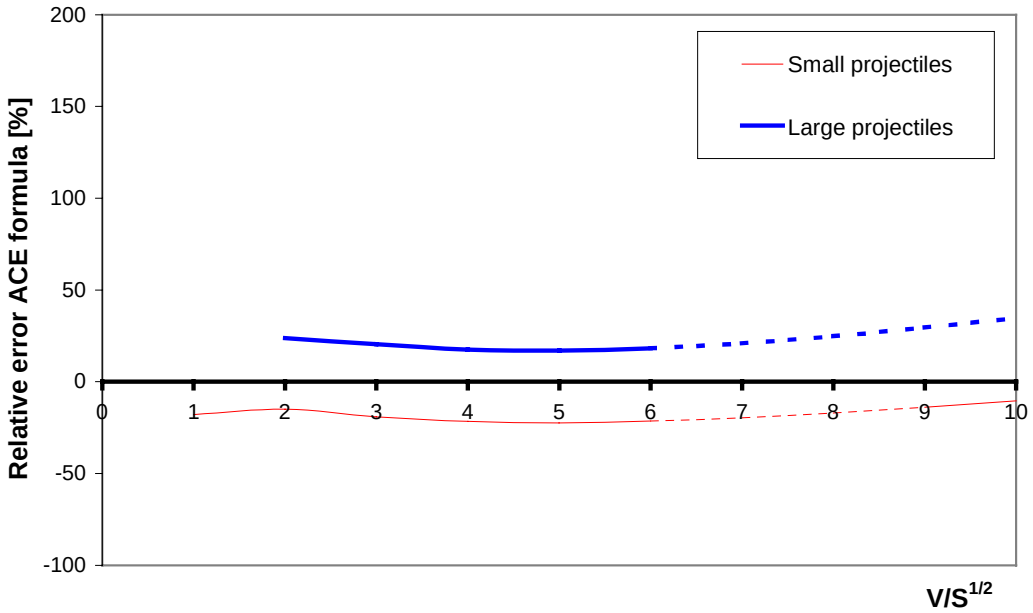

Figure 6.3: Relative error between the ACE formula and Forrestal's formula

6.2.2 Bergman's formula

Bergman's formula seems to be mainly based on projectiles with low impact velocities. For small projectiles with impact velocities $V/\sqrt{S}$ between 2 and 4, the deviation from Forrestal's formula is less than 35 %. For these projectiles, Bergman's formula can be used somewhere outside the range of the impact velocity, but for impact velocities $V/\sqrt{S}$ greater than 10, the deviation from Forrestal's formula is growing, due to the increasing velocity exponent. For the large projectiles, only one impact velocity was used

in the experiments (300 m/s; corresponding to $V/\sqrt{S}$ equal to 1.8). In this case, the deviation from Forrestal's formula is approximately 30 %. For larger impact velocities, the deviation from Forrestal's formula is almost constant, but is increasing for impact velocities larger than the inflection point velocity.

The velocity exponent in Bergman's formula depends on the impact velocity, and this exponent can be shown to be greater than 1.5 for all impact velocities giving penetration depths larger than 3.5 calibres.

This means that Bergman's formula is very sensitive to the impact velocity, especially when applied to high impact velocities. The value of *M/N* in the data behind Bergman's formula is between 25 and 39, and all experiments were performed with impact velocities below the inflection point velocity. This explains the fact that the velocity exponent in Bergman's formula is an increasing function of the impact velocity.

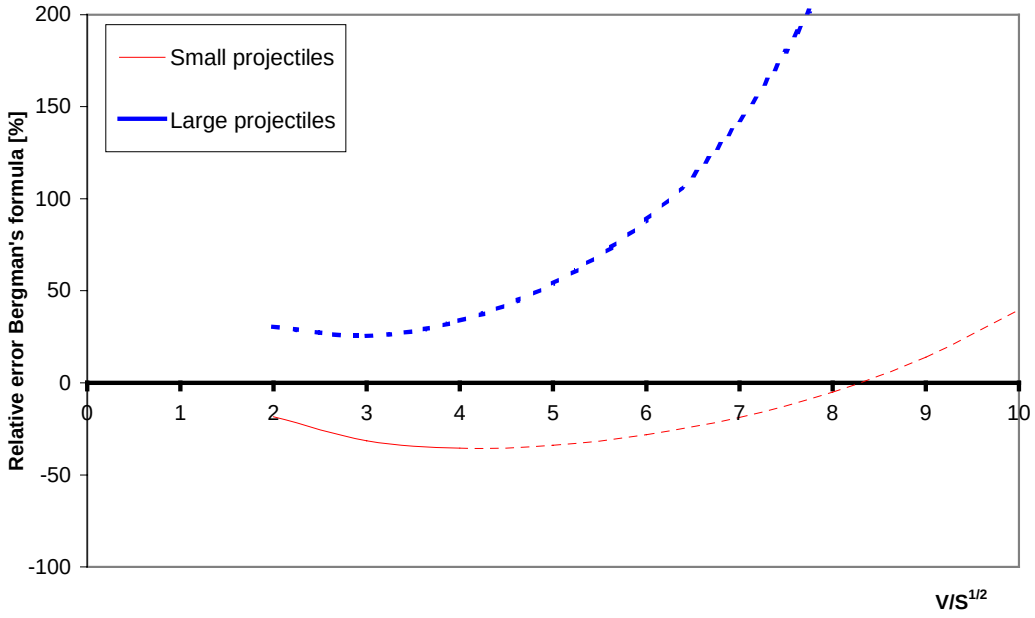

Figure 6.4: Relative error between Bergman's formula and Forrestal's formula.

6.2.3 Bernard's formula

The least square approximations of Bernard's formula give velocity exponents larger than 1.5 for both the small and large projectiles. Bernard's formula gives a linear relationship between the penetration depth and the impact velocity, but this is predefined, and not a result from curce fitting procedures.

For small projectiles, the deviation from Forrestal's formula is less than 20 % for all velocities used in the experiments behind Bernard's formula. In fact, the experimental data against concrete targets taken from (4) are all performed with the smaller projectiles, as shown in Table 5.15.

For the large projectiles, the deviation from Forrestal's formula is less than 20 % for $V/\sqrt{S} > 7$. The larger projectiles were all fired against rock targets, and the comparison in Figure 13 shows that more investigation of the material model for rock targets in Forrestal's formula, i.e. further research on the *S*-factor, must be performed.

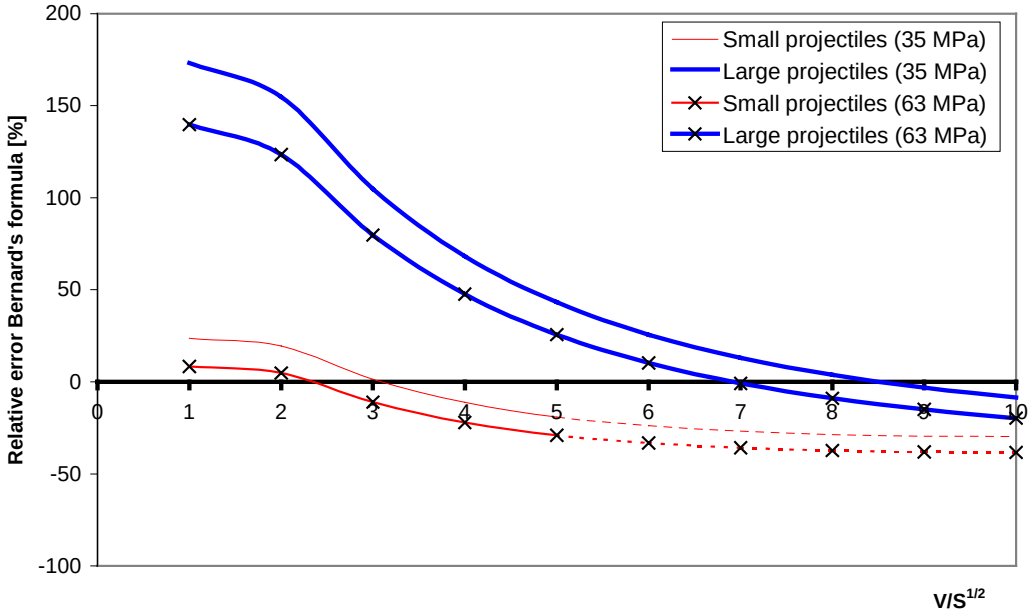

Figure 6.5: Relative error between Bernard's formula and Forrestal's formula.

6.2.4 Hughes' formula

Hughes' formula seems to be the only formula which is based on experiments with approximately contant value of *M/N*, which again should result in good agreement to Forrestal's formula. Figure 6.6 shows that this is indeed the case. The deviation from Forrestal's formula is less than 20 % in all cases, and the formulas are almost identical for experiments against low strength concrete (σ_c = 22.1 MPa).

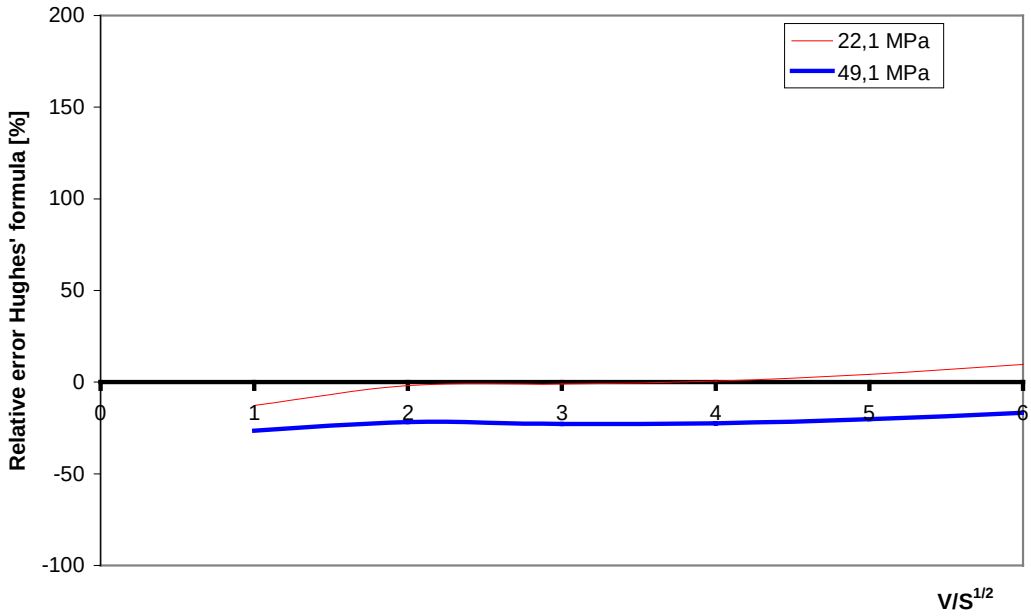

Figure 6.6: Relative error between Hughes' formula and Forrestal's formula.

6.2.5 NDRC formula

The NDRC formula is based on experiments with 12.7 mm projectiles, i.e. the value of *M/N* is constant. These data are compared to Forrestal's formula in Figure 13. As shown in Figure 5, the velocity exponent in the resulting empirical formula can vary from 1.5 to 1.8, depending on the velocity range of the experiments. The velocity exponent in the NDRC formula is 1.8.

6.2.6 TBAA formula

The velocity exponent for the TBAA formula depends on the compressive strength of the concrete. For high strength concrete (σ_c = 69.1 MPa), the velocity exponent is approximately 1.0, and for the low strength concrete, n = 2.0. The scaled impact velocity $V/S^{1/2}$ is reduced when the compressive strength is increased, which indicates higher velocity exponent for experiments with high strength concrete.

The only way to explain the velocity exponent in the TBAA formula is that the experiments against high strength concrete were performed with high impact velocities. Against the low strength concrete, the impact velocity must have been in the lower range for the impact velocity.

The velocity exponent given by the least square approximations correspond to compressive strengths between 25 MPa and 35 MPa, which is the compressive strength of standard concrete.

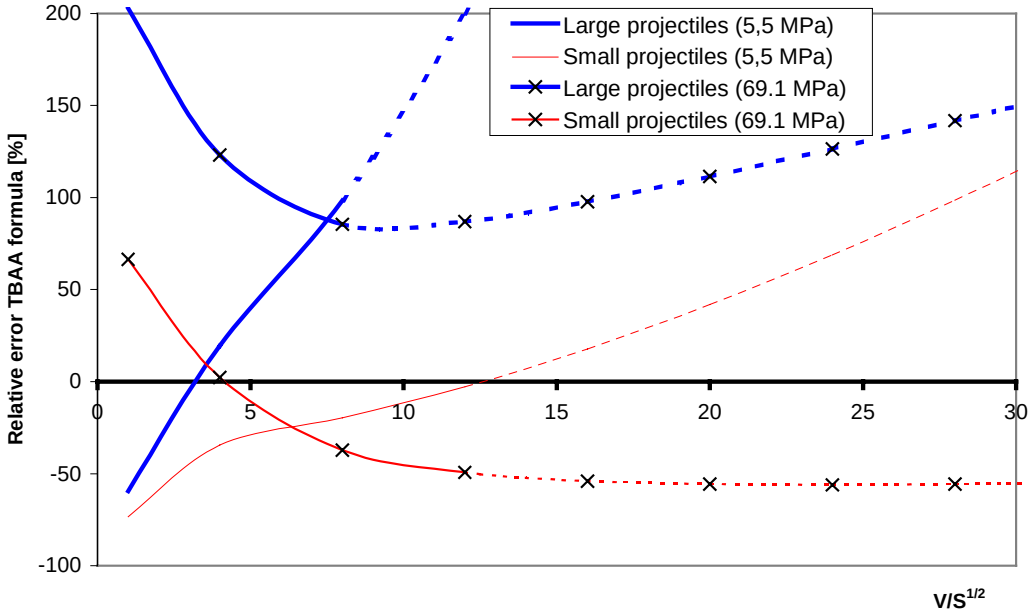

Figure 6.7: Relative error between the TBAA formula and Forrestal's formula.

6.2.7 Young's formula

The velocity exponent in Young's formula is 1.0, which is in best agreement with the least square approximation for the large projectiles. From Figure 12, the deviation from Forrestal's formula is also best for the large projectiles within the range of the impact velocity.

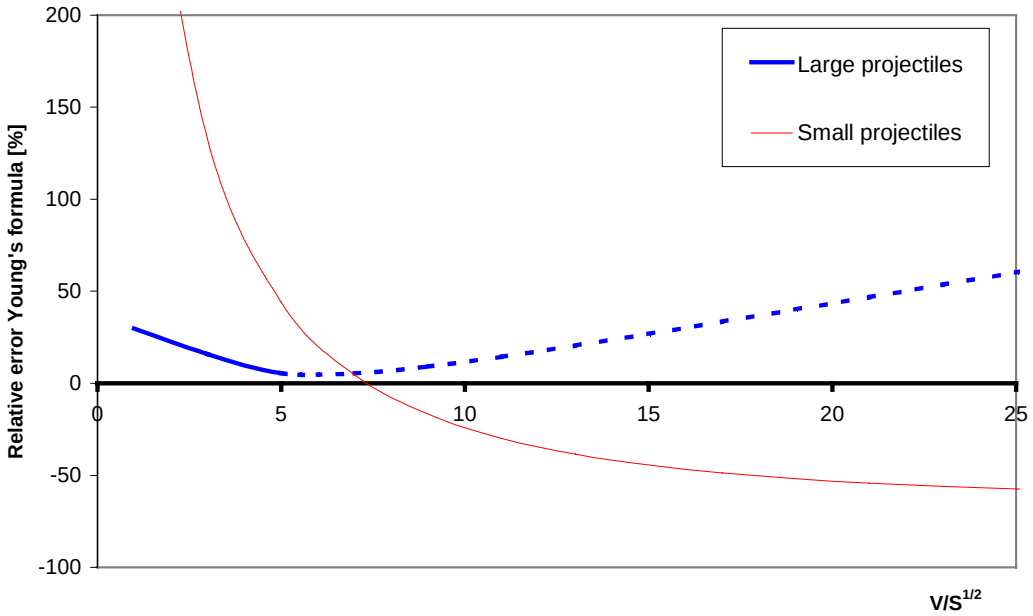

Figure 6.8: Relative error between Young's formula and Forrestal's formula.

7 APPLICATION TO MODERN WEAPONS

In Teland (22), the empirical equations were applied to different kinds of modern weapons. However, the formulas were used outside the range of validity, especially when applying them to HPC targets. In Chapter 5, Forrestal's formula was shown to be valid for compressive strengths up to 200 MPa. The penetration depth into concrete for the three weapons studied in (22) is in Figure 7.1 shown as a function of the compressive strength. In Table 7.1, the data of the actual weapons are listed.

Table 7.1: Data for different modern weapons.

	GBU-28	Modern weapon I	Modern weapon II
Mass [kg]	2040	500	113
Diameter [mm]	368	250	155
Impact velocity [m/s]	500	500	1500
Length to diameter ratio	11	10	10

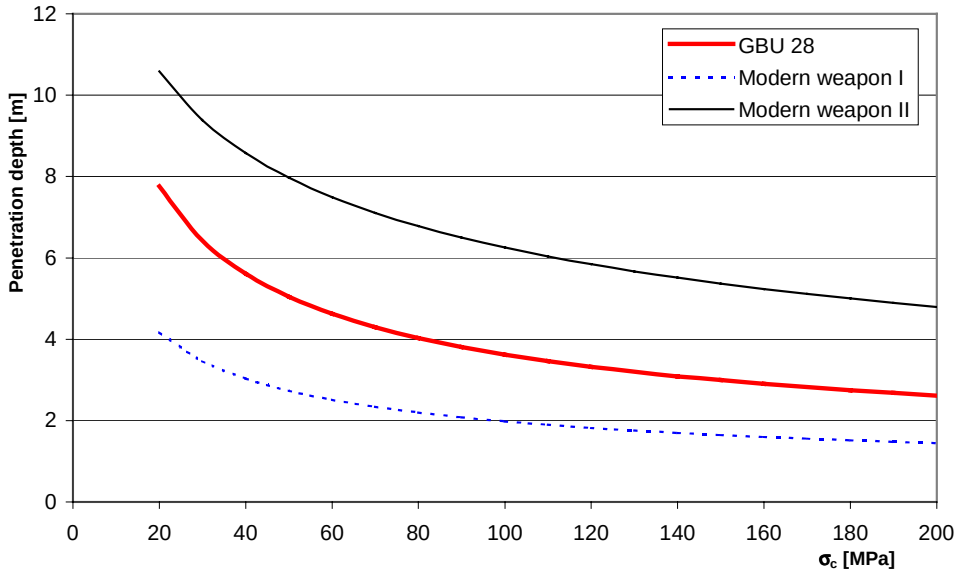

Figure 7.1: Penetration depth for 3 different modern weapons as function of the compressive strength of the concrete target calculated by Forrestal's formula.

8 SUMMARY AND CONCLUSIONS

Forrestal's formula can be written on a non-dimensional form, giving the non-dimensional penetration depth as a function of non-dimensional impact velocity and the non-dimensional mass. For each value of the non-dimensional mass, there is a corresponding relationship between the penetration depth and impact velocity. This may explain the

difference between the existying empirical formulas, as they may be based on experiments with different projectiles.

As seen in Figures 6.3 – 6.8, the relative error between the different empirical formulas and Forrestal's formula are zero somewhere in the range of the parameters used in the experiments. This may indicate which projectiles that were used in the experiments. Most empirical formulas seem to be based on experiments with different values of *M/N* in their data sets. As shown in Section 4.5, Forrestal's formula gives one formula for each value of *M/N*, which means that the resulting empirical formula strongly depends on the range of the other parameters used in the experiments. Hughes' formula is the only formula based on experimental data unknown to us, where a constant value of *M/N* ($M/N \approx 30$) seems to have been used. It gives best agreement with Forrestal's formula compared to all the other empirical formulas.

Experiments with constant value of *M/N* can also result in different empirical equations. As shown in Section 6.1.1, the velocity exponent strongly depends on the range of the impact velocity, especially if this range is below the inflection point velocity given by Equation (4.13). For the empirical equations analysed here, this seems to be the case.

Since the velocity exponent is very sensitive to the impact velocity range used, one should be very careful when using the empirical formulas for high velocities. Especially for Bergman's formula, where the velocity exponent is an increasing function of the impact velocity. This formula is therefore not recommended for high impact velocities.

Bernard's formula and the NDRC formula are based on experiments with constant value of *M/N*, and in these cases the deviation from Forrestal's formula is less than 20 %. Both formulas are based on experiments with approximately the same value of *M/N*, but the velocity exponents are 1.0 for Bernard's formula and 1.8 for the NDRC formula. From Table 3, there should only be a slight difference in the velocity exponent using a least square technique, which is due to the impact velocity range. However, Bernard (4) has chosen a linear relationship between the penetration depth and impact velocity, i.e. it is not found from curve fitting procedures. This explains the apparently large difference between two empirical formulas that "should have been" almost identical.

The analysis in this paper shows the importance of using non-dimensional parameters in planning and performing experiments. Since Forrestal's formula results in one formula for for each value of *M/N*, experiments with different values of *M/N* should not be used to produce a single empirical formula. This was probably done for the majority of the existing empirical formulas, which explains why they have turned out to be so different.

APPENDIX

A DERIVATION OF FORRESTAL'S PENETRATION EQUATION

The force acting on the projectile is, by Forrestal , assumed to be

$$f = \begin{cases} cx & x/d < 2 \\ \frac{\pi d^2}{4}\left(S\sigma_c + N\rho v^2\right) & x/d > 2 \end{cases} \tag{A.1}$$

Where c is a constant which will be determined later. Equation (A.1) shows that the force is proportional to the penetration depth for x/d < 2, and a function of the impact velocity for x/d > 2. To determine the penetration depth, the penetration depth is first calculated for x/d > 2, using the initial conditions $x_0 = 2$ og $v_0 = v_1$. The velocity v_1 will be determined later. Newtons 2. law gives

$$m\frac{\partial^2 x}{\partial t^2} = -\sigma_c d^2 \frac{\pi S}{4}\left(1 + \frac{N}{M}\frac{V^2}{S}\right) \tag{A.2}$$

By recalling the non-dimensional quantities given by Equation (2.1),

$$X = \frac{x}{d} \quad V = \sqrt{\frac{m}{d^3\sigma_c}}v \quad M = \frac{m}{d^3\rho_t} \quad N = g(x/d)$$

and including the non-dimensional time

$$T = \sqrt{\frac{d\sigma_c}{m}}t \tag{A.3}$$

the following differential equation arise:

$$\frac{\partial^2 X}{\partial T^2} = -\frac{\pi S}{4}\left(1 + \frac{N}{M}\frac{V^2}{S}\right) \tag{A.4}$$

The non-dimensional time T has been defined in such way that $\frac{\partial X}{\partial T} = V$.

By rewriting the acceleration as

$$\frac{\partial^2 X}{\partial T^2} = \frac{\partial V}{\partial T} = \frac{\partial V}{\partial X}\frac{\partial X}{\partial T} = V\frac{\partial V}{\partial X} \tag{A.5}$$

the differential equation (A.5) can be written on separable form

$$-\frac{VdV}{1+\frac{N}{M}\frac{V^2}{S}}=\frac{\pi}{4}SdX \tag{A.6}$$

Equation (A.6) is solved by integrating from $V=V_1$ to $V=0$. This gives the following relationship between the scaled penetration depth X and V_1:

$$X=\frac{2}{\pi}\frac{M}{N}\ln\left(1+\frac{N}{M}\frac{V_1^2}{S}\right)+2 \tag{A.7}$$

The velocity V_1 is then found from the equation

$$m\frac{\partial^2 x}{\partial t^2}=-\sigma_c d^2 cx \tag{A.8}$$

Transforming to non-dimensional quantities, the penetration depth as a function of time is found from

$$\frac{\partial^2 X}{\partial T^2}+cX=0 \qquad X(0)=0 \qquad \frac{\partial X}{\partial T}(0)=V \tag{A.9}$$

which yields

$$X(T)=\frac{1}{\sqrt{c}}V\sin\sqrt{c}T \tag{A.10}$$

Defining the time $T=T_1$ where X=2 and $V=V_1$, giving

$$X(T_1)=\frac{1}{\sqrt{c}}V\sin\sqrt{c}T_1=2$$

$$\frac{\partial X}{\partial T}(T_1)=V\cos\sqrt{c}T_1=V\sqrt{1-\sin^2\sqrt{c}T_1}=V_1 \tag{A.11}$$

Continuity at $T=T_1$ gives

$$c=\frac{\pi S}{8}\left(1+\frac{N}{M}\frac{V_1^2}{S}\right) \tag{A.12}$$

Combining Equation (A.11) and (A.12), gives the velocity when X=2 as a function of the impact velocity:

$$V_1^2=\frac{V^2-\pi/2\,S}{1+\pi/2\,N/M} \tag{A.13}$$

Inserting this expression into Equation (A.7), the scaled penetration depth as a function of impact velocity is finally found to be

$$\frac{x}{d} = \frac{2}{\pi}\frac{M}{N}\ln\left[\frac{{}^{M}\!/_{N} + \hat{V}^{2}}{\left({}^{\pi}\!/_{2} + {}^{M}\!/_{N}\right)}\right] + 2 \qquad \hat{V} > \sqrt{\frac{\pi}{2}} \tag{A.14}$$

For flat nosed projectiles, the force acting on the projectile is given by cavity expansion theory from t=0. This means that the maximum penetration depth is found by integrating Equation (A.6), giving following modified formula:

$$\left(\frac{x}{d}\right)_{\text{mod}} = \frac{2}{\pi}\frac{M}{N}\ln\left[1 + \frac{N}{M}\frac{V^{2}}{S}\right] \tag{A.14b}$$

References

(1) Adeli H, Amin M (1985): Local effects of impactors on concrete structures, Nuclear Engineering and design 88, 301-317

(2) Baker W E, Westine P S, Dodge F T (1973): Similarity methods in engineering dynamics, Hayden Book Company Inc

(3) Bergman S G A (1950): Inträngning av panserbrytande projectiler och bomber i armerad betong, FortF Rapport B2, Stockholm, Sweden

(4) Bernard R S (1976): Empirical analysis of projectile penetration in rock, US Army Waterways Experiment station, Paper AEWES-MP-S-77-16

(5) Berthelsen P A (1999): Cavity expansion og penetrasjonsmekanikk - materialmodeller og numeriske løsningsmetoder, FFI/RAPPORT-99/04260

(6) Beth R A: Concrete penetration, NDRC report no A-319, OSRD Report No 4856

(7) Forrestal M J, Luk V K (1992): Penetration into soil targets, *Int J Impact Eng* **12**, 427-444

(8) Forrestal M J, Altman B S, Cargile J D, Hanchak S J (1994): An empirical equation for penetration depth of ogive nose projectiles into concrete targets, *Int J Impact Eng* **15**, 4, 395-405

(9) Forrestal M J, Frew D J, Hanchak S J, Brar N S (1996): Penetration of grout and concrete targets with ogive-nose steel projectiles, *Int J Impact Eng* **18**, 5, 465-476.

(10) Fraser R D G: Penetration of projectiles into concrete and soil, Working paper AW(87)WP13.

(11) Frew D J, Hanchak S J, Green M L, Forrestal M J (1998): Penetration of concrete targets with ogive-nosed steel rods, *Int J Impact Eng* **21**, 6, 489-497

(12) Haldar A, Miller F J (1982): Penetration depth in concrete for nondeformable missiles, *Nuclear Engineering and Design* **71**, 79-88

(13) Hellström, K G (1986): Jämnförelse mellan nogre olika formler för beräkning av projektilers inträngning i betong, FortF Rapport C6, Eskilstuna, Sweden

(14) Hughes G (1984): Hard missile impact on reinforced concrete, *Nuclear Engineering and Design* **77**, 23-35

(15) Kar A K (1978): Local effects on tornado-generated missiles, *J Struct Div ASCE* **104**, ST5, 809-816

(16) Langberg H, Markeset G (1999): High performance concrete - penetration resistance and material development, *Proceedings of the 9th international symposium on interaction of the effects of munitions with structures, 3-7 May 1999, Berlin Germany*, 299-306

(17) Luk V K, Forrestal M J (1987): Penetration into semi-infinite reinforced concrete targets with sperical and ogival nose projectiles, *Int J Impact Eng* **6**, 4, 291-301

(18) NDRC: Effects of impact and explosion, summary of technical Report of division 2, National Defence Research Commitee, Vol 1, Washington D C

(19) Sjøl H, Teland J A, Kaldheim Ø (1998): Penetrasjon i betong med 12 mm prosjektiler, FFI/NOTAT-98/04392

(20) Sjøl H, Teland J A (1999): Extension and improvement of the NDRC formula based on experiments with 12 mm steel projectiles against concrete targets, *Proceedings of the 9th international symposium on interaction of the effects of munition with structures, 3-7 May 1999, Berlin Germany*, 275-282

(21) Teland J A (1997): A review of empirical equations for missile impact effects on concrete, FFI/RAPPORT-97/05856

(22) Teland J A (1998): En undersøkelse av penetrasjonsevnen til moderne våpen ved bruk av empiriske formler, FFI/RAPPORT-98/04328

(23) Teland J A (1999): A review of analytical penetration mechanics, FFI/RAPPORT-99/01264

(24) Teland J A, Sjøl H (1999): An examination and reinterpretation of experimental data behind various empirical equations for penetration into concrete, *Proceedings of the 9th international symposium on interaction of the effects of munition with structures, 3-7 May 1999, Berlin Germany*, 267-274

(25) Tolsch N A, Buskowitch A V (1947): Penetration and crater volume in various kinds of rocks as dependent on caliber, mass, striking velocity of projectile, BRL Report No 641, October 1947

(26) Vretblad B (1988): Penetration of projectiles in concrete according to FortH 1, *Proceedings from the workshop on weapon penetration into hard targets, Norwegian Defence Research Establishment, 30-31 May 1988*

(27) Young C V (1996): Class notes - Seminar on penetration mechanics, Trondheim March 1996

DISTRIBUTION LIST

FFIBM **Dato:** 29 juni 2000

RAPPORTTYPE (KRYSS AV)	RAPPORT NR.	REFERANSE	RAPPORTENS DATO
X RAPP ☐ NOTAT ☐ RR	99/04415	FFIBM/766/130	29 juni 2000
RAPPORTENS BESKYTTELSESGRAD		ANTALL EKS UTSTEDT	ANTALL SIDER
Unclassified		54	48
RAPPORTENS TITTEL		FORFATTER(E)	
PREDICTION OF CONCRETE PENETRATION USING FORRESTAL'S FORMULA		SJØL Henrik, TELAND Jan Arild	
FORDELING GODKJENT AV FORSKNINGSSJEF:		FORDELING GODKJENT AV AVDELINGSSJEF:	

EKSTERN FORDELING

ANTALL	EKS NR	TIL
1		FBT/S
1		Helge Langberg
1		Gro Markeset
1		Leif Riis
1		Anders Carlberg
3		Johan Magnusson
1		FOA
		S-14725 TUMBA, Sverige
1		Ingvar Anglevik
1		HKV/KRI Plan/Anläggning
		SE-10785 STOCKHOLM
		Sverige
1		Bjørn Lindberg
1		Forv-M
		S-63189 ESKILSTUNA
		Sverige
1		Jaap Weerheijm
1		Cyril Wentzel
1		TNO
		Lange Kleinweg 137
		P.O Box 45
		2280 AA RIJSWIJK, Nederland
1		Cathy O'Carroll
1		Jim Sheridan
1		DERA
		X107, Barnes Wallis Building
		Farnborough
		Hampshire GU14 0LX
		England

INTERN FORDELING

ANTALL	EKS NR	TIL
14		FFI-Bibl
1		Adm direktør/stabssjef
1		FFIE
1		FFISYS
5		FFIBM
1		Eirik Svinsås, FFIBM
1		Jan Arild Teland, FFIBM
1		Svein Rollvik, FFIS
1		Bjarne Haugstad, FFIBM
1		Haakon Fykse, FFIBM
1		John F. Moxnes, FFIBM
1		Ove Dullum, FFIBM
1		Svein E. Martinussen, FFIBM
4		Henrik Sjøl, FFIBM
1		Harald H. Soleng, FFIBM
		FFI-veven

FFI-K1 Retningslinjer for fordeling og forsendelse er gitt i Oraklet, Bind I, Bestemmelser om publikasjoner for Forsvarets forskningsinstitutt, pkt 2 og 5. Benytt ny side om nødvendig.